

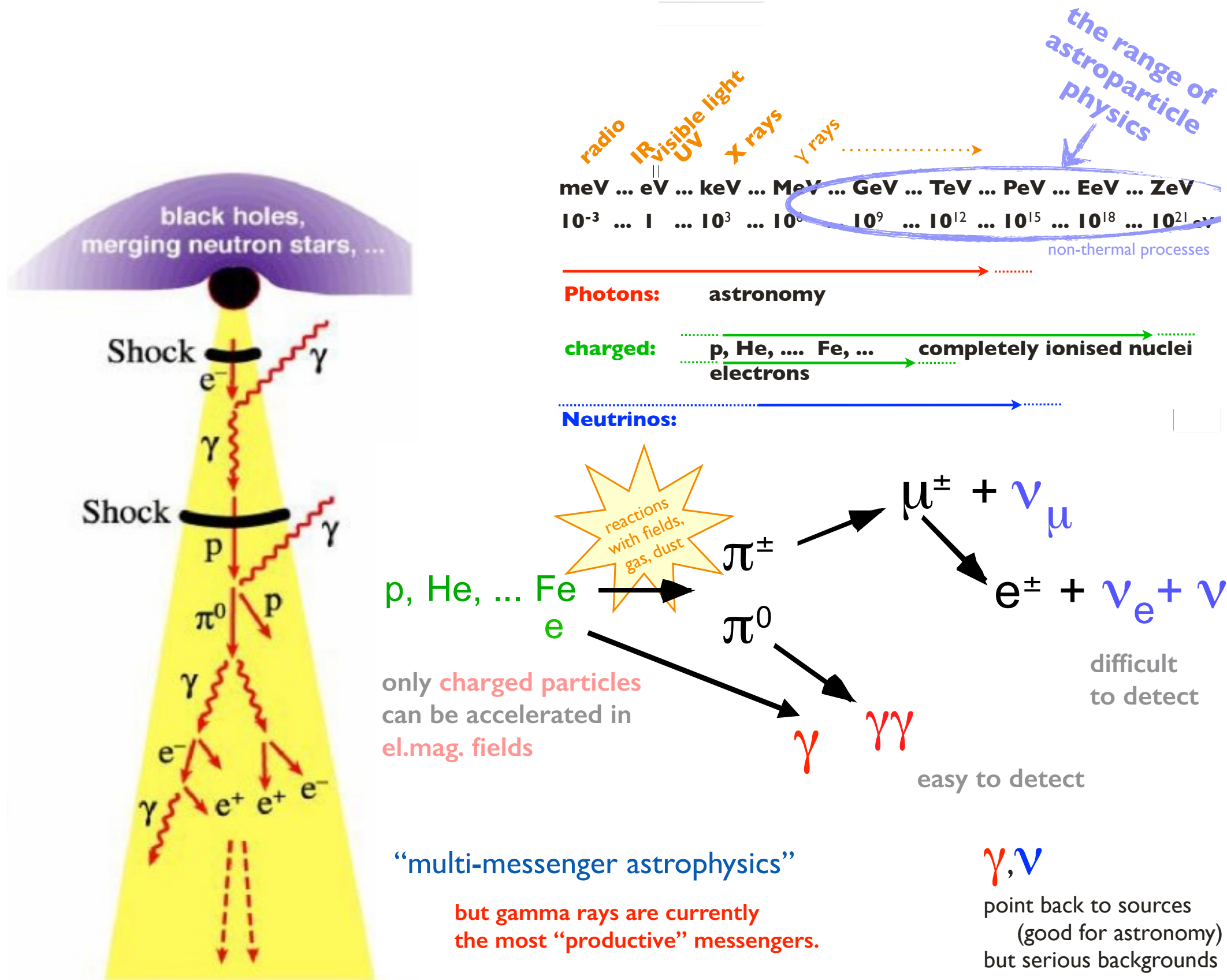
# Towards locating the ultra-high energy cosmic ray accelerators?



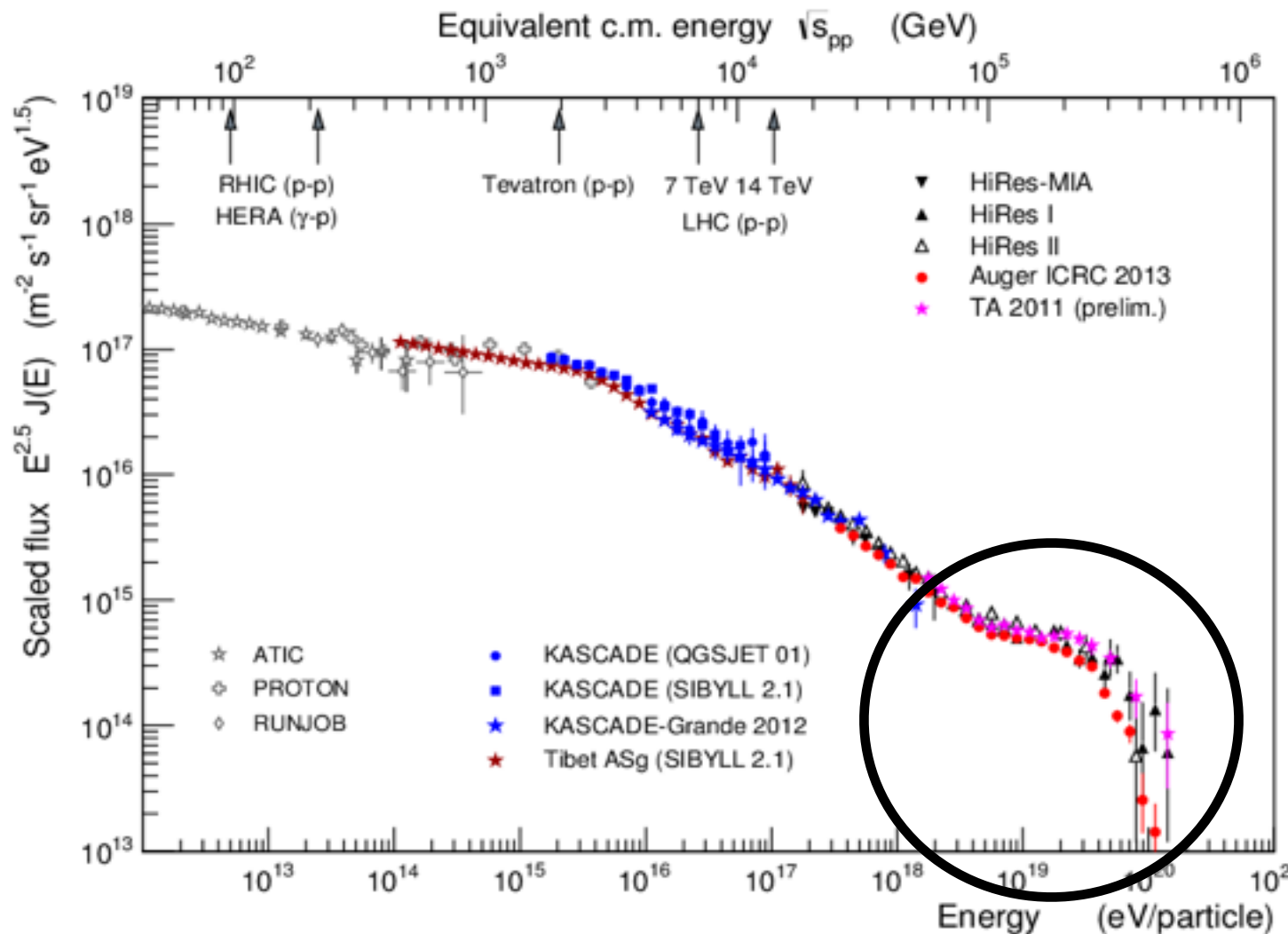
O. Deligny (CNRS/IN2P3 - IPN Orsay)

- i)* Introduction**
- ii)* The Pierre Auger Observatory**
- iii)* The energy spectrum and mass composition:  
the rise of the rigidity-dependent scenario for the  
maximal acceleration energy**
- iv)* Extragalactic pattern of cosmic-ray arrival  
directions above  $8 \times 10^{18}$  eV**
- v)* Correlation of UHECR arrival directions  
with the flux pattern of nearby star-forming  
galaxies**

# Generic cosmic-ray accelerators



# Ultra-high energy cosmic rays: contemporary questions

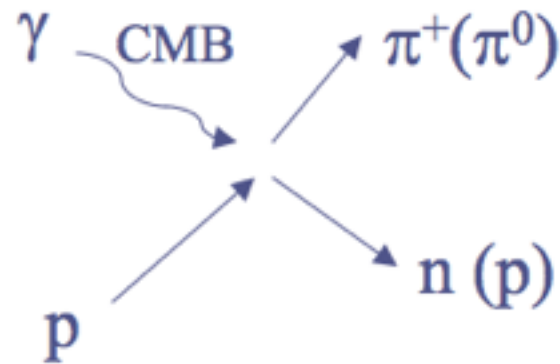


- Gal/xGal transition?
- Origin of the ankle?
- Origin of the UHE steepening?
- Composition at UHE?
- Sources?

NB: From neutrinos/photons upper limits, the bulk of UHECRs are accelerated particles in astrophysical objects

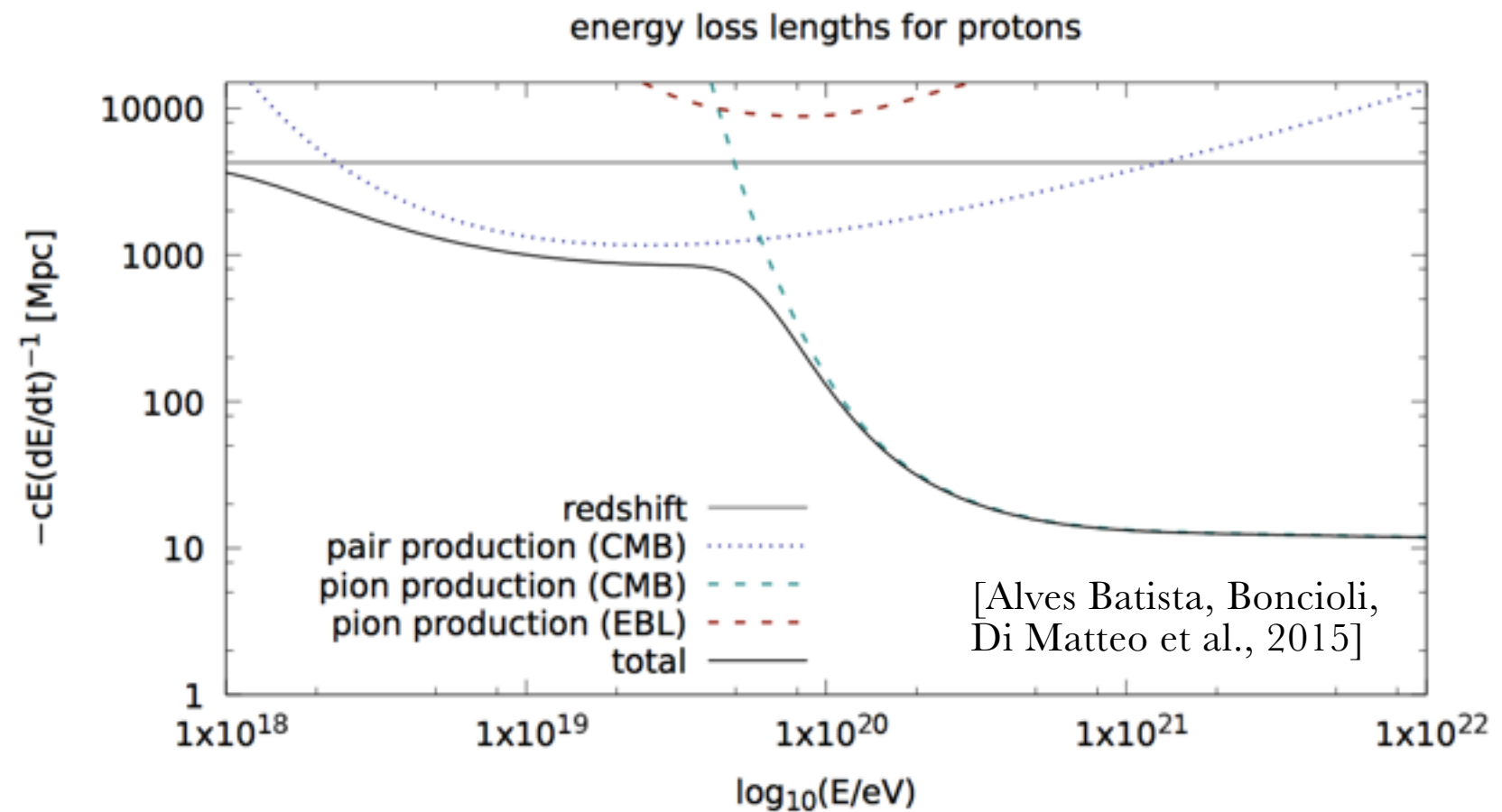
# The GZK cutoff

Example with protons



$$\varepsilon_\gamma > \frac{m_\pi m_p}{\varepsilon_p} \sim 10^{-3} \varepsilon_{20}^{-1} \text{ eV} \Rightarrow n_\gamma \sim \frac{400}{\text{cm}^3} \exp\left[1 - \frac{3}{\varepsilon_{20}}\right]$$

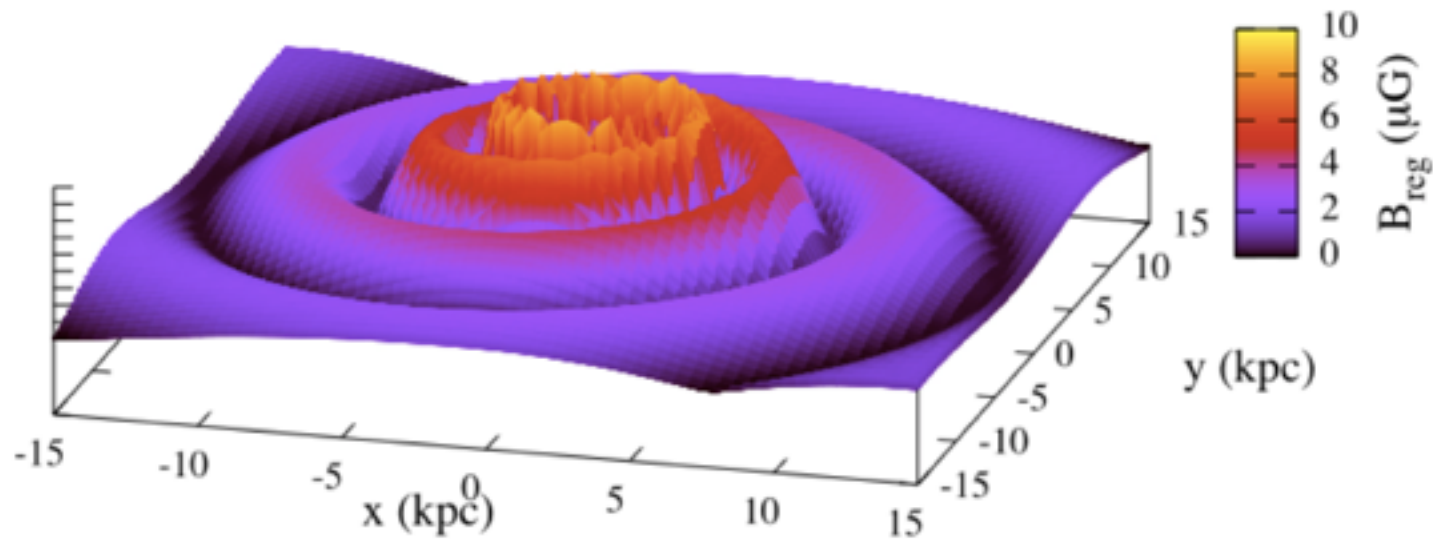
$$\lambda_E \sim \frac{m_p}{m_\pi} \frac{1}{n_\gamma \sigma_{\gamma p}} \sim 11 \exp\left[\frac{3}{\varepsilon_{20}} - 1\right] \text{ Mpc}$$



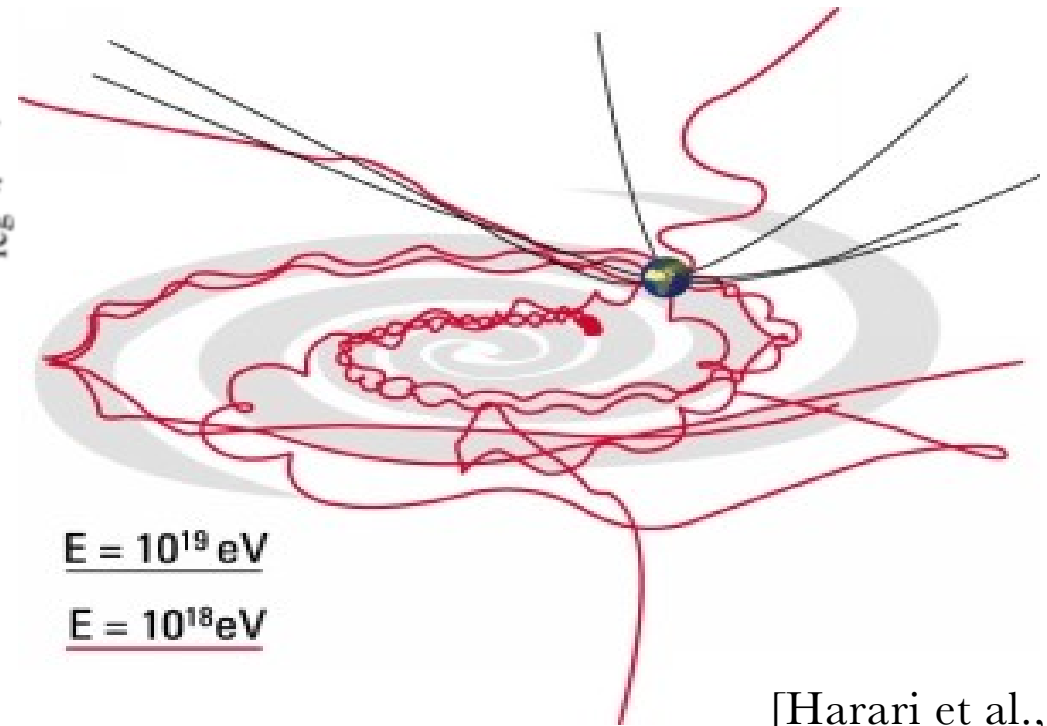
Same phenomenon with nuclei (photo-disintegration)

➔ Sudden reduction of the CR horizon at UHE

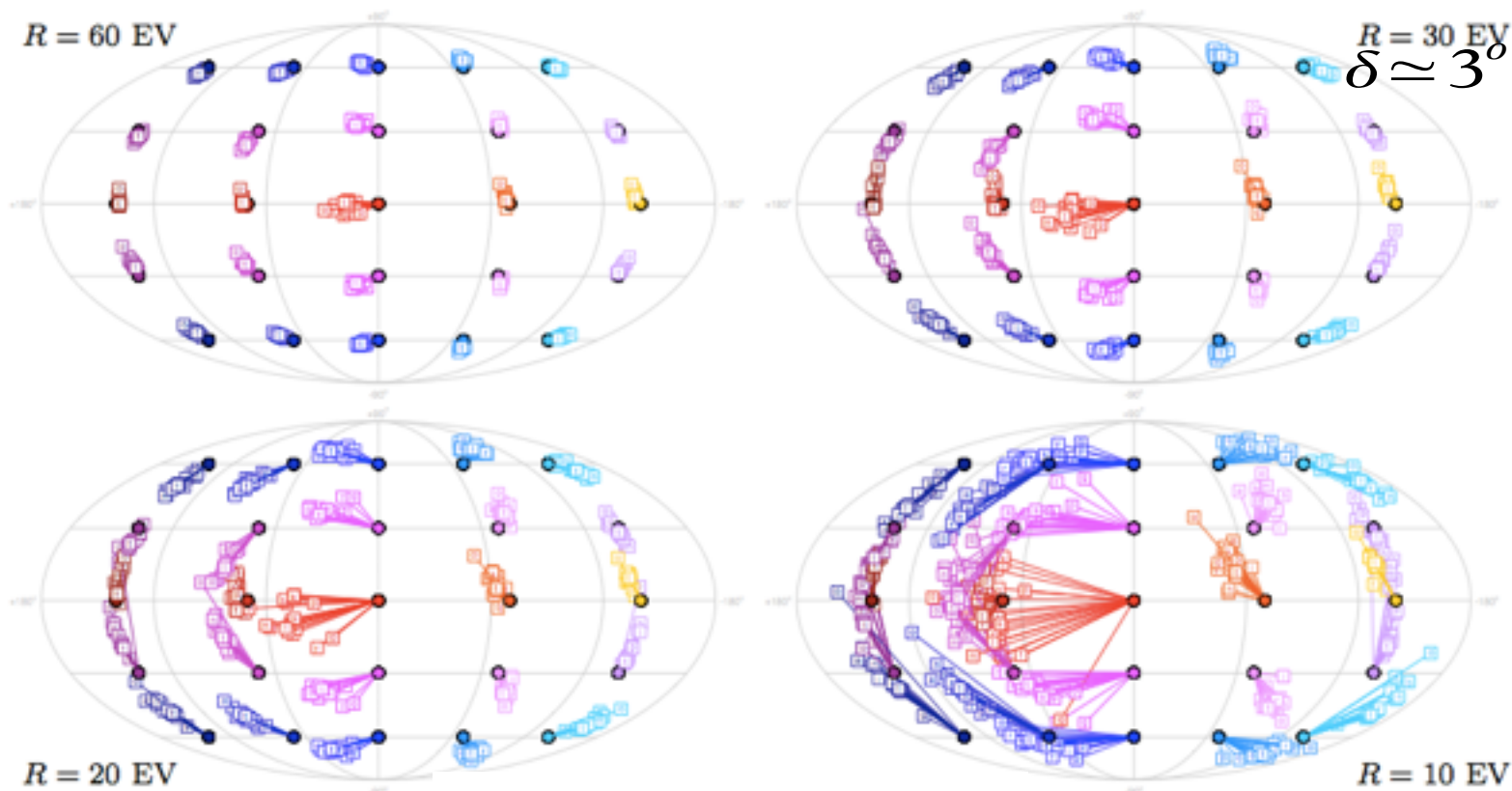
# Magnetic deflections



[Jansson & Farrar 2012]



[Harari et al., 1999]



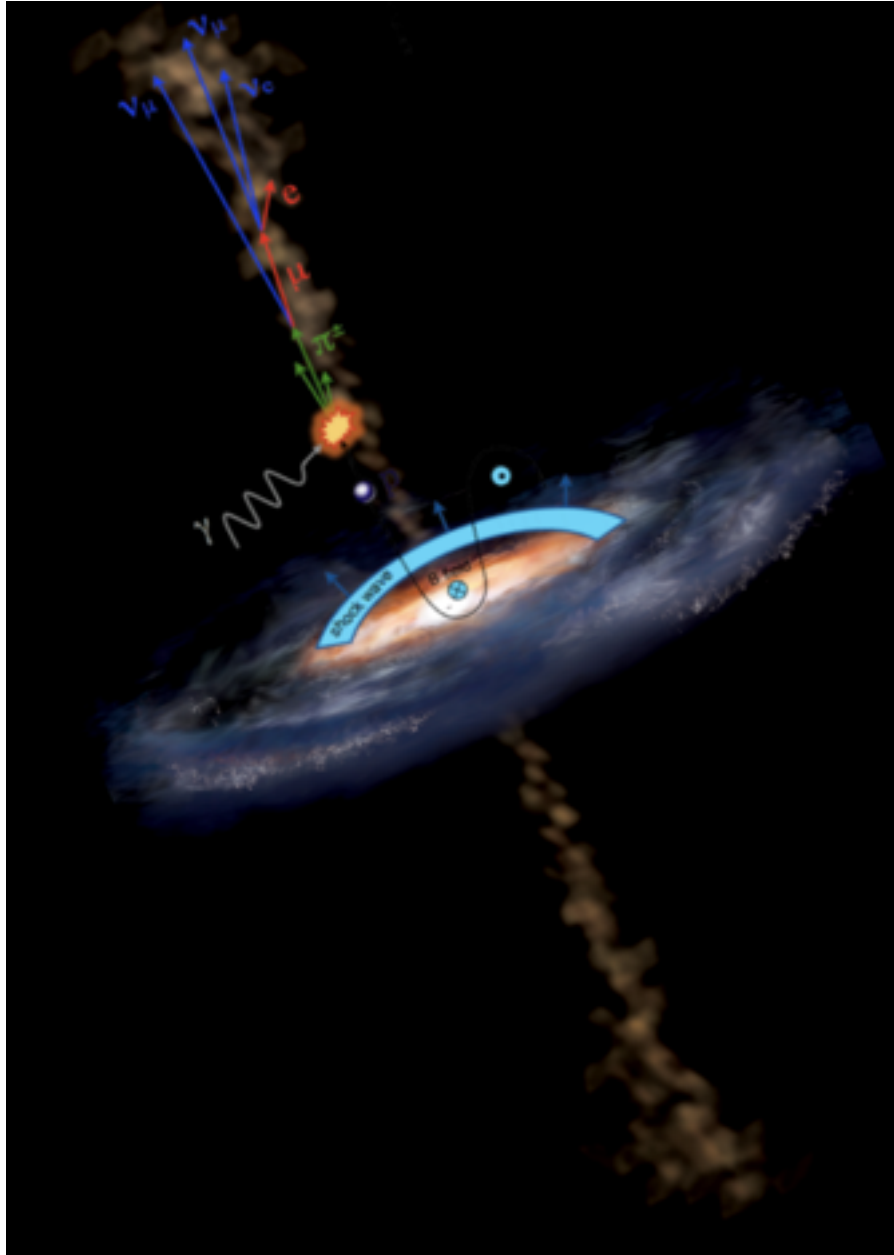
[Unger & Farrar 2017]

At UHE, CRs may be rigid enough to point back to their sources within a few degrees

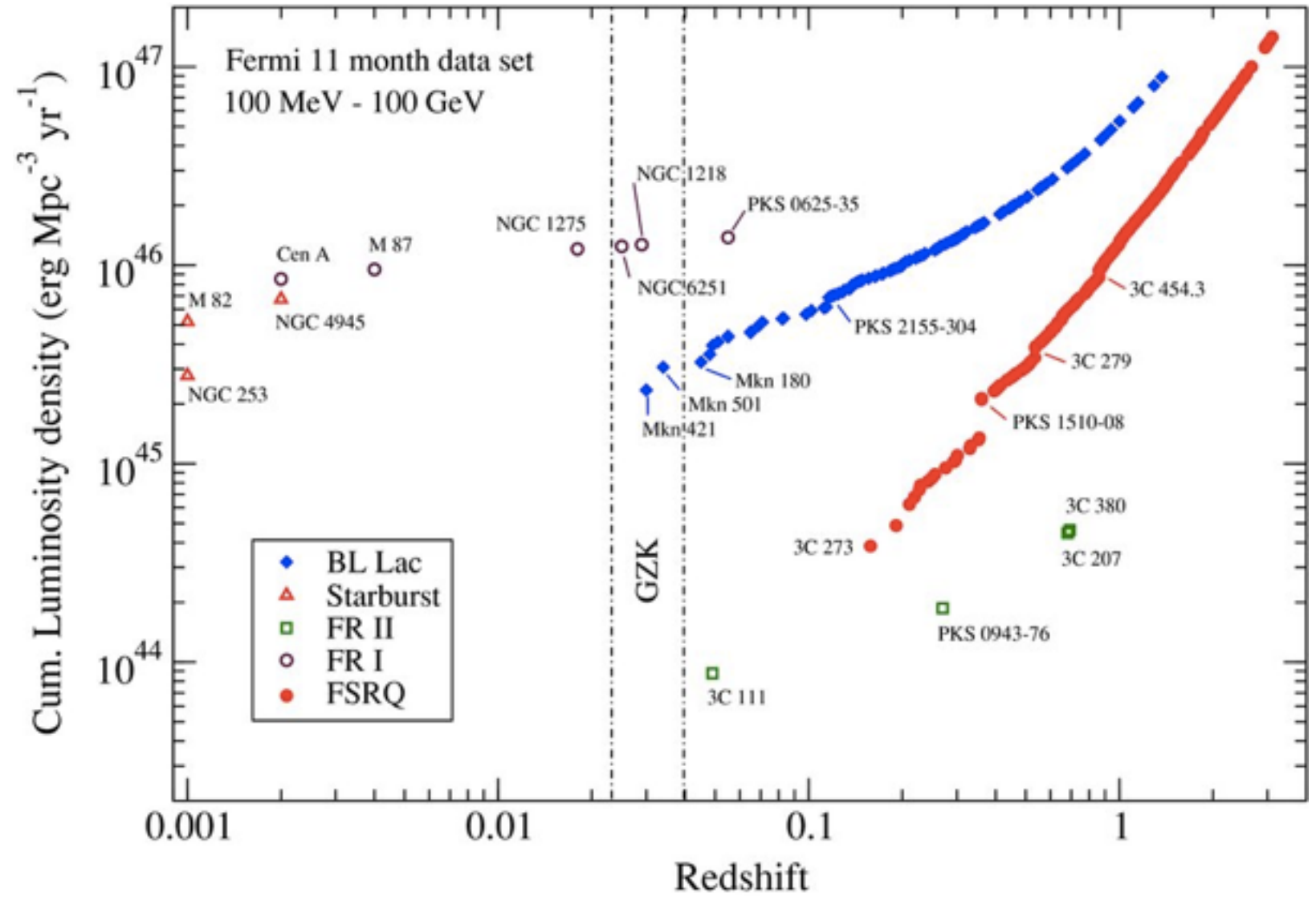
+ Reduced horizon

➔ Possibility to identify nearby sources?

# Multi-messenger connection?



[Dermer & Razzaque 2010]

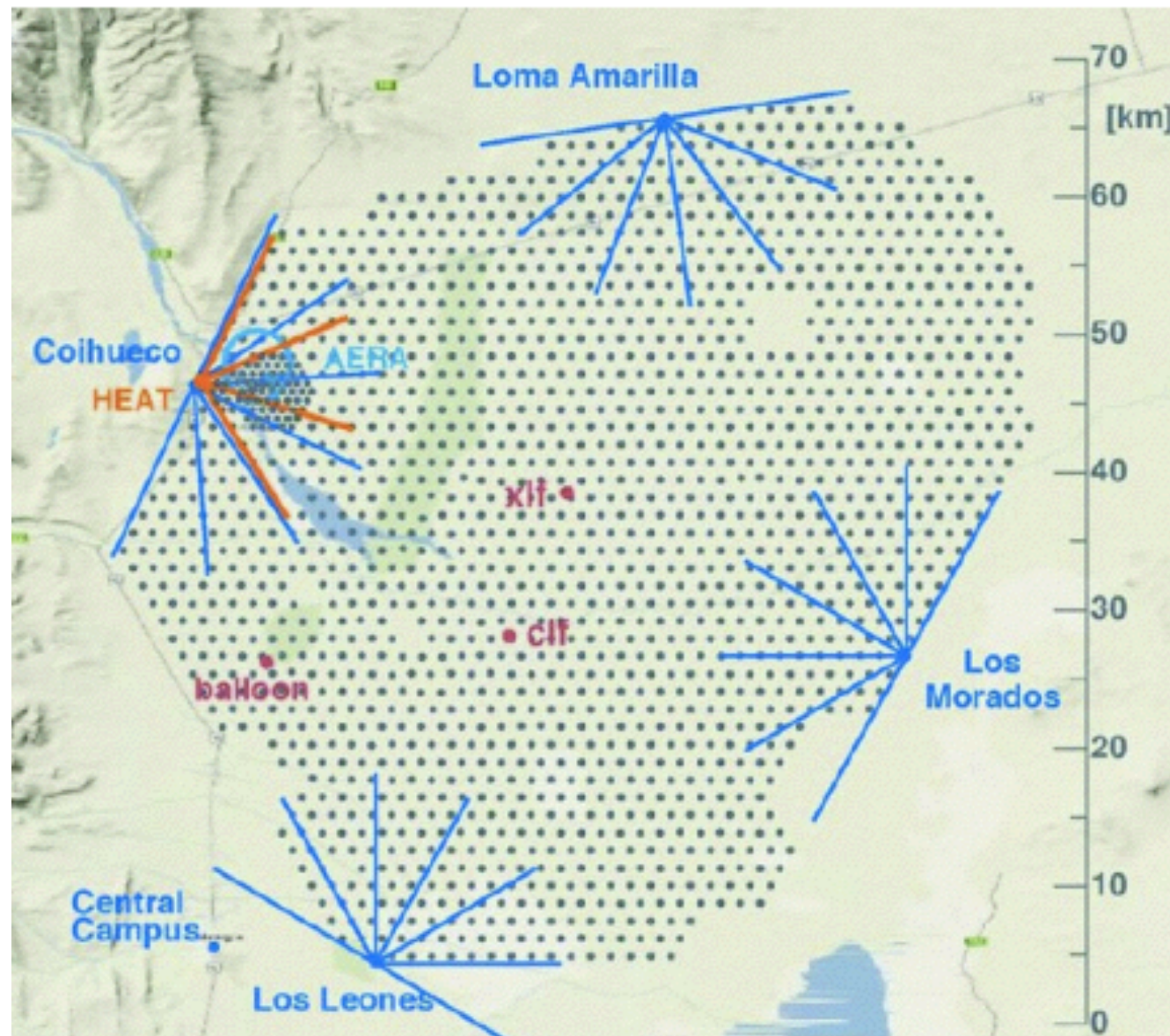




## *ii)* **The Pierre Auger Observatory**

# The Pierre Auger Observatory

Located in Argentina, province of Mendoza



## Hybrid detector:

- **Surface detector array (SD):**

- **SD-1500:**

- 1660 spaced by 1.5 km  
~ 3000 km<sup>2</sup>

- **SD-750:**

- 49 spaced by 750 m  
~ 24 km<sup>2</sup>

- **Fluorescence detector (FD):**

- 27 fluorescence telescopes in 5 buildings

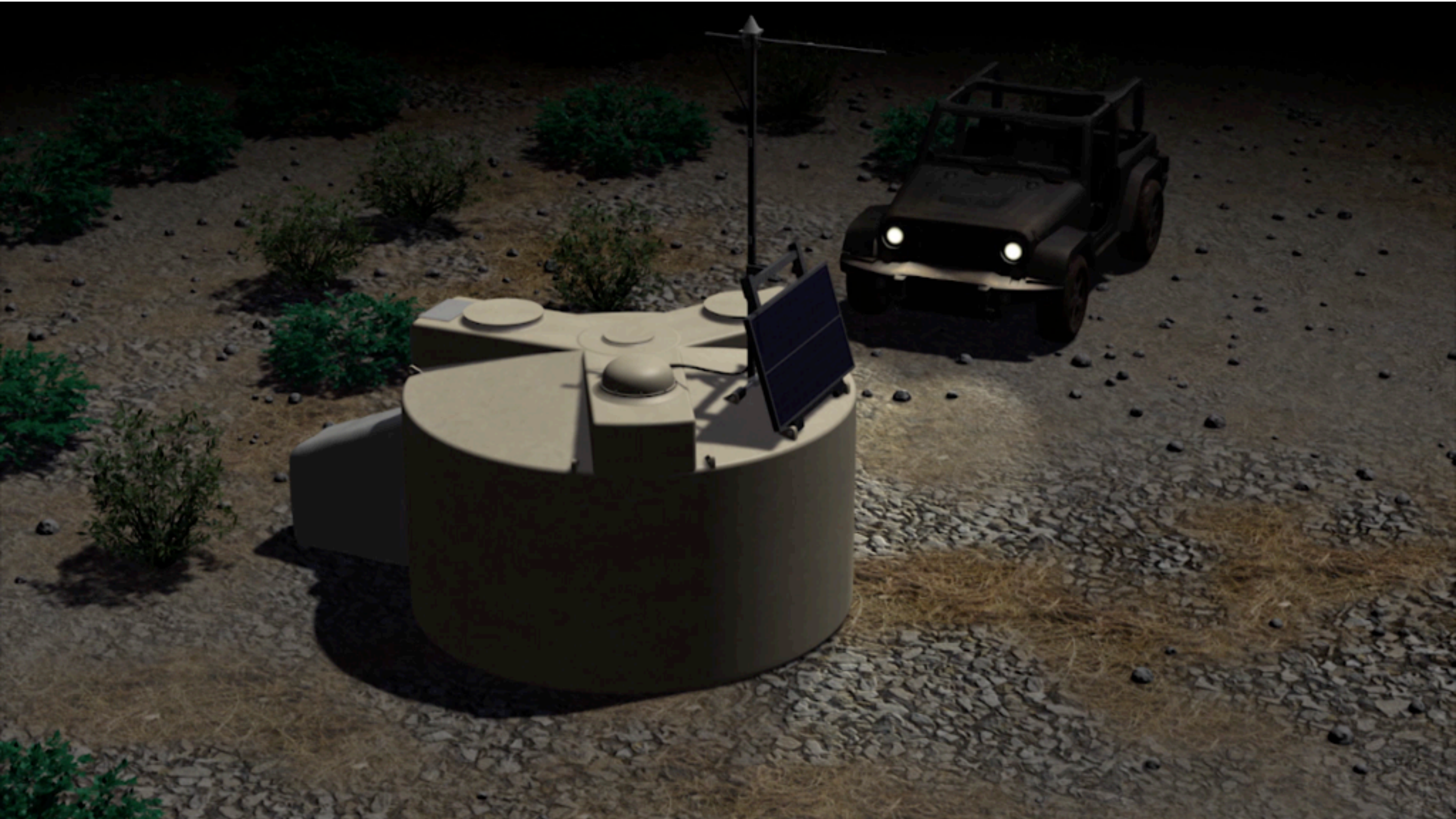
# Surface detectors

---

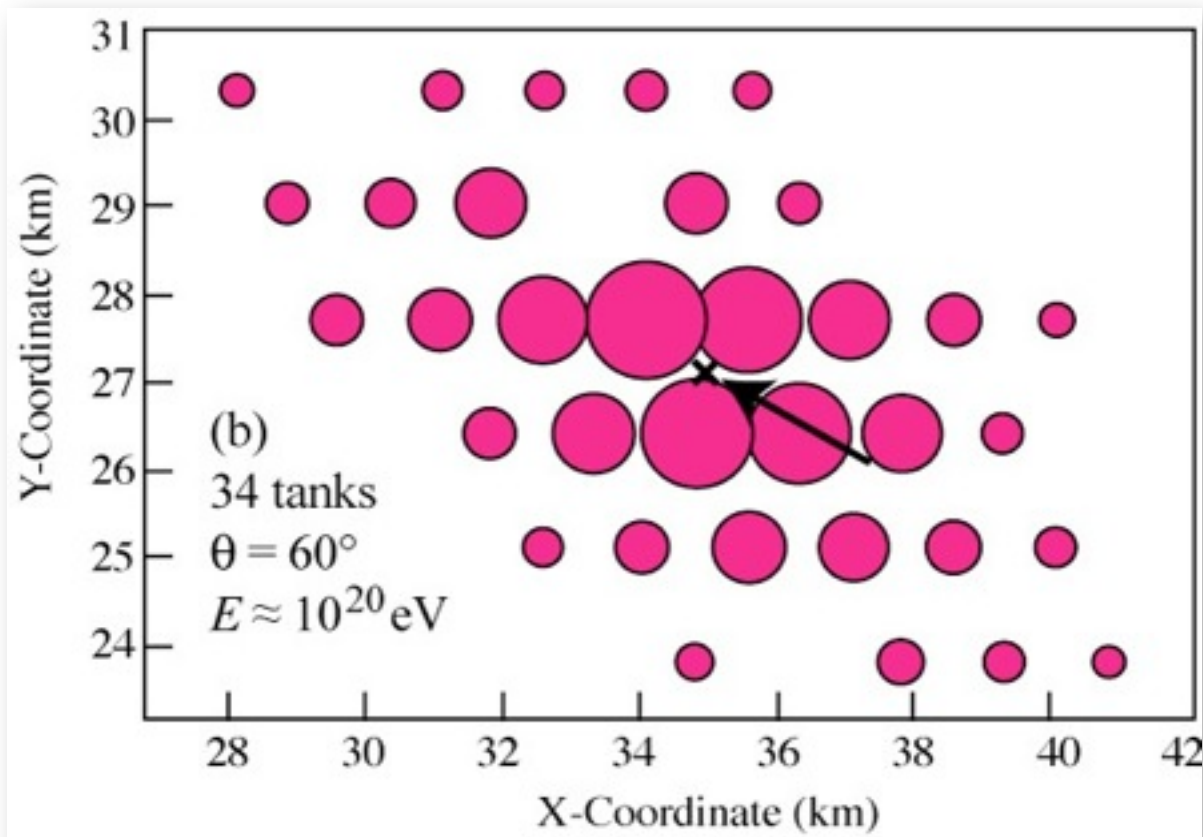


# Surface detectors

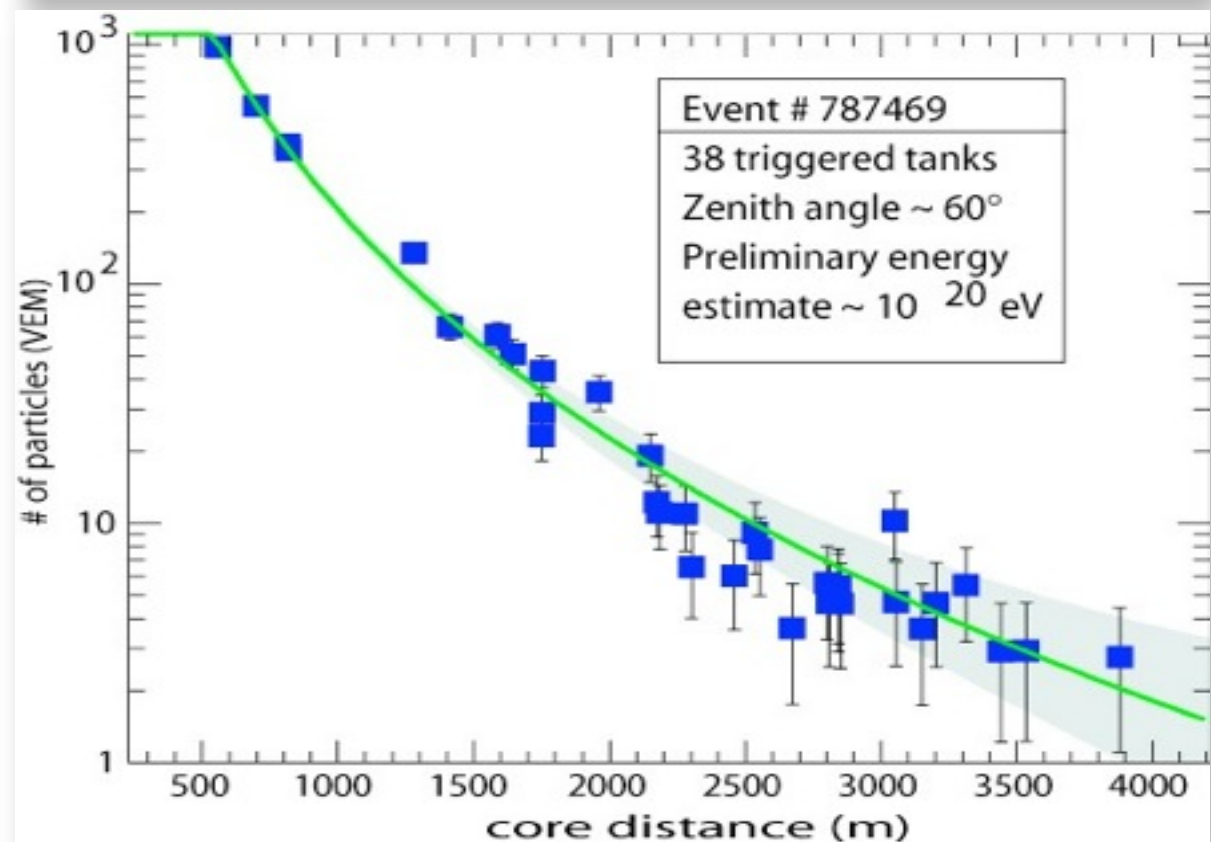
---



# Surface detectors



Footprint of the shower at ground = lateral sampling



arrival direction +  
'size' of the shower

$\sim 100\%$  duty cycle

# Fluorescence detectors

---

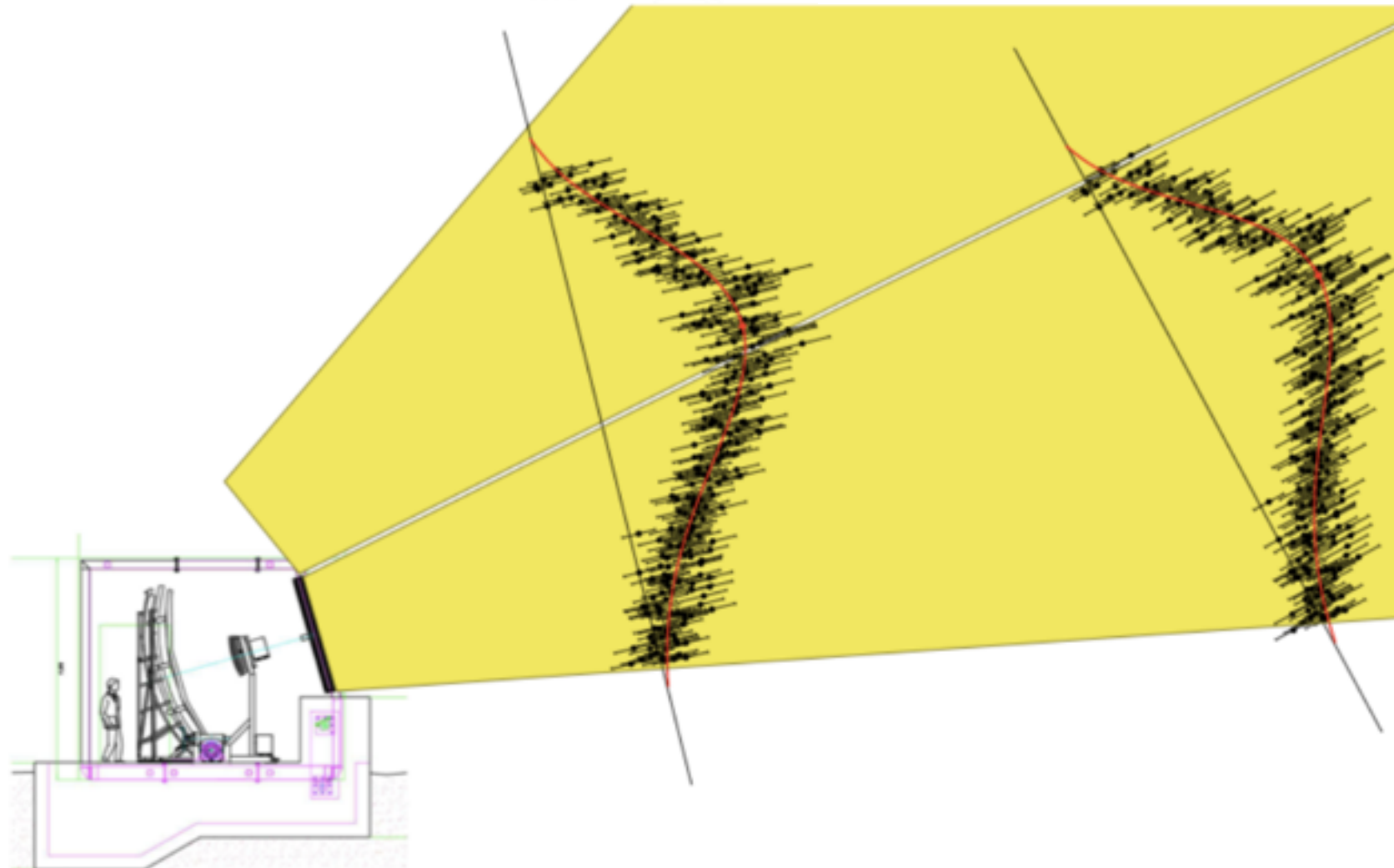
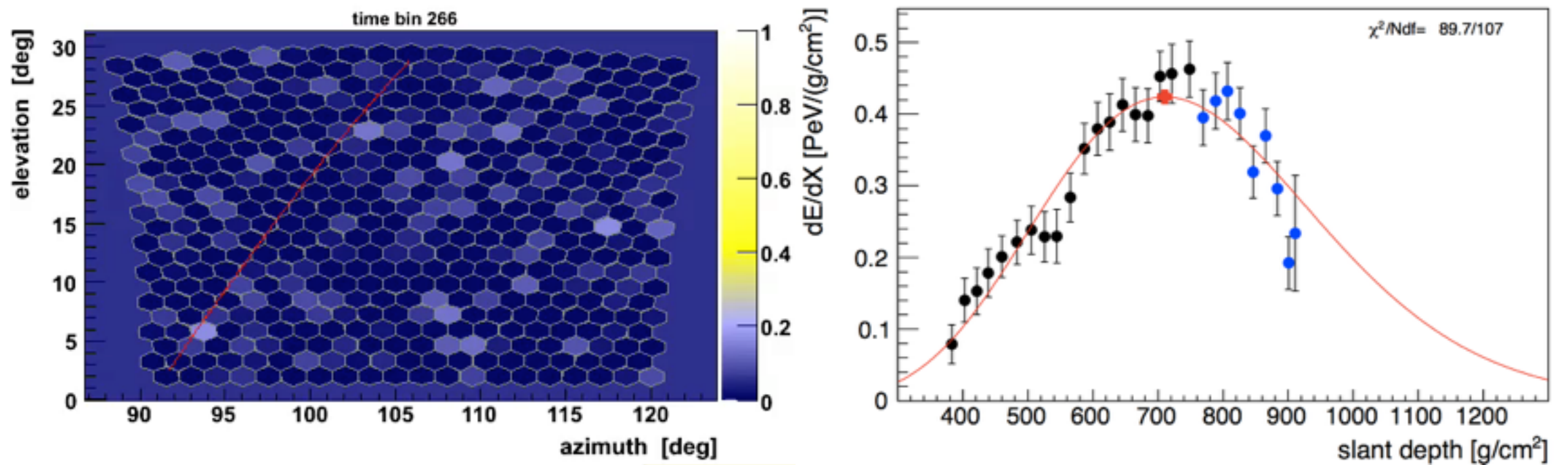


# Fluorescence detectors

---



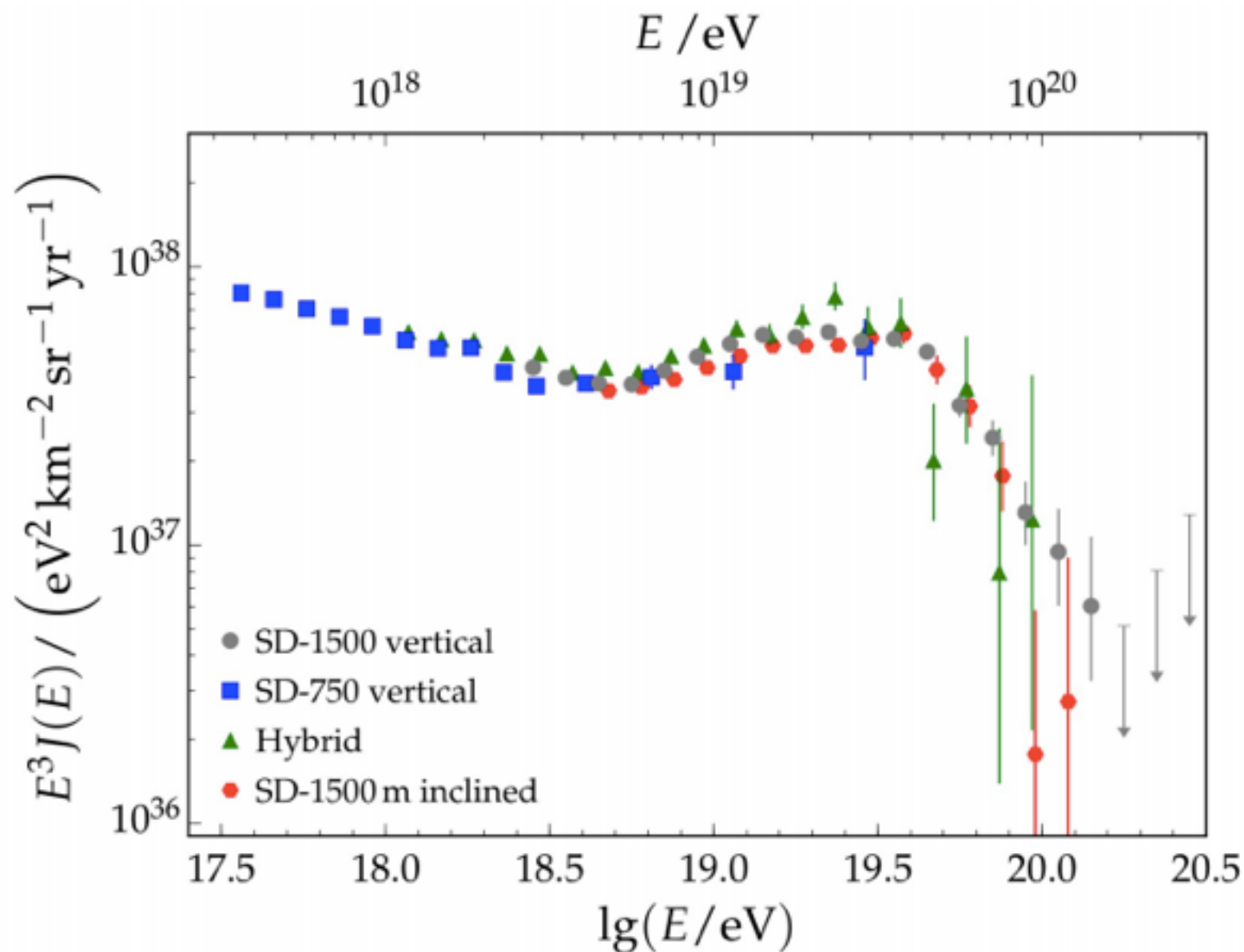
# Fluorescence detectors



~13% duty cycle

***iii)* The energy spectrum and mass composition: the rise of the rigidity-dependent scenario for the maximal acceleration energy**

# Energy spectrum measurements



**Energy systematic uncertainty**  
(dominated by the FD energy scale)

14%

**Hybrid**  
11680 events  
 $\log(E) > 18$   
Exposure: 1946  $\text{km}^2 \text{ sr yr}$  @  $10^{19}$  eV  
(25% increase wrt 2015)

Flux uncertainty: 10%

**SD-1500 vertical**  
183332 events  
 $\log(E) > 18.4$   
Exposure: 51588  $\text{km}^2 \text{ sr yr}$   
(20% increase wrt 2015)

Flux uncertainty: 5.8%

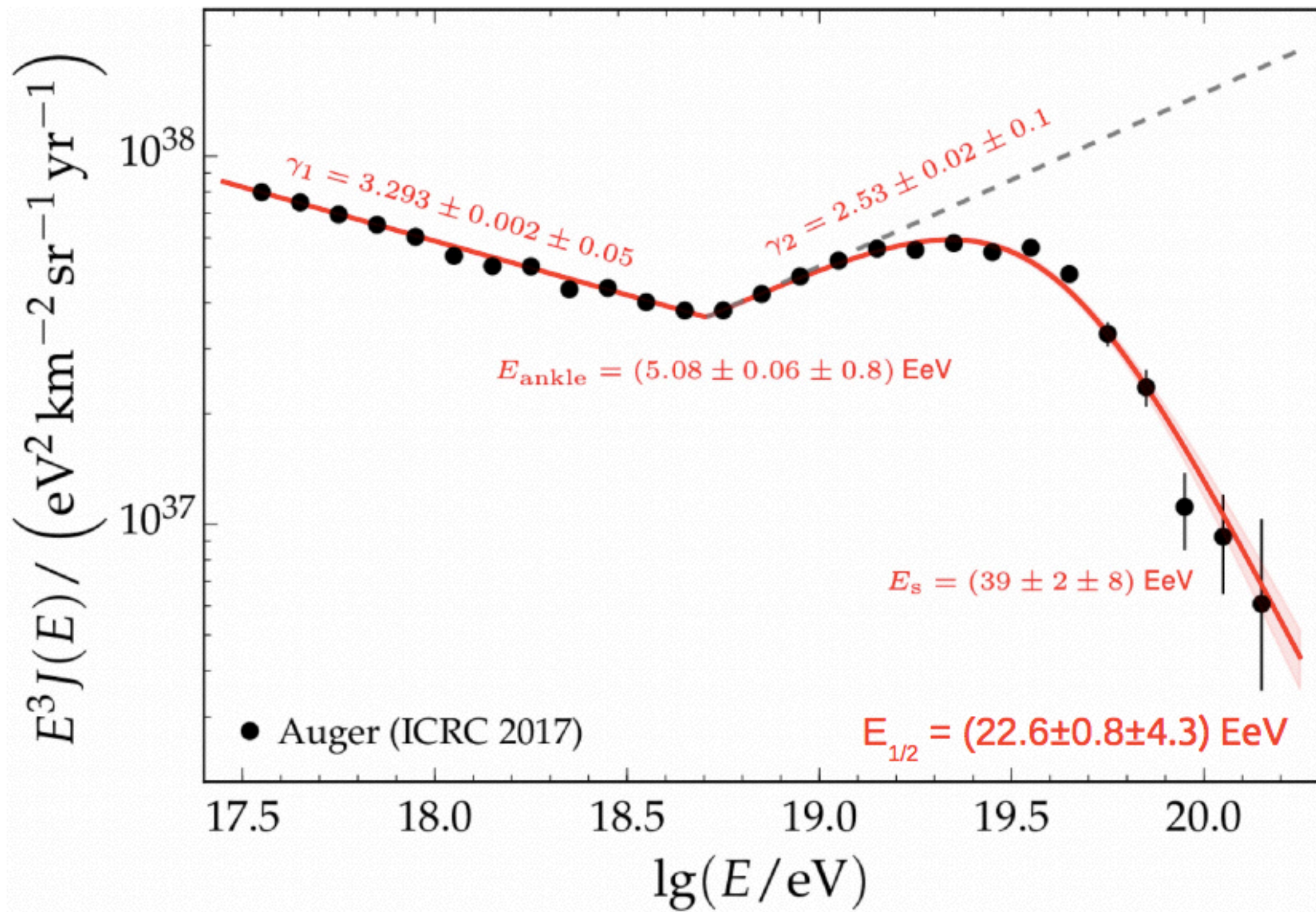
**SD-750 vertical**  
87402 events  
 $\log(E) > 17.5$   
Exposure 228  $\text{km}^2 \text{ sr yr}$   
(50% increase wrt 2015)

Flux uncertainty 14 – 7% @ (0.3 – 3) EeV

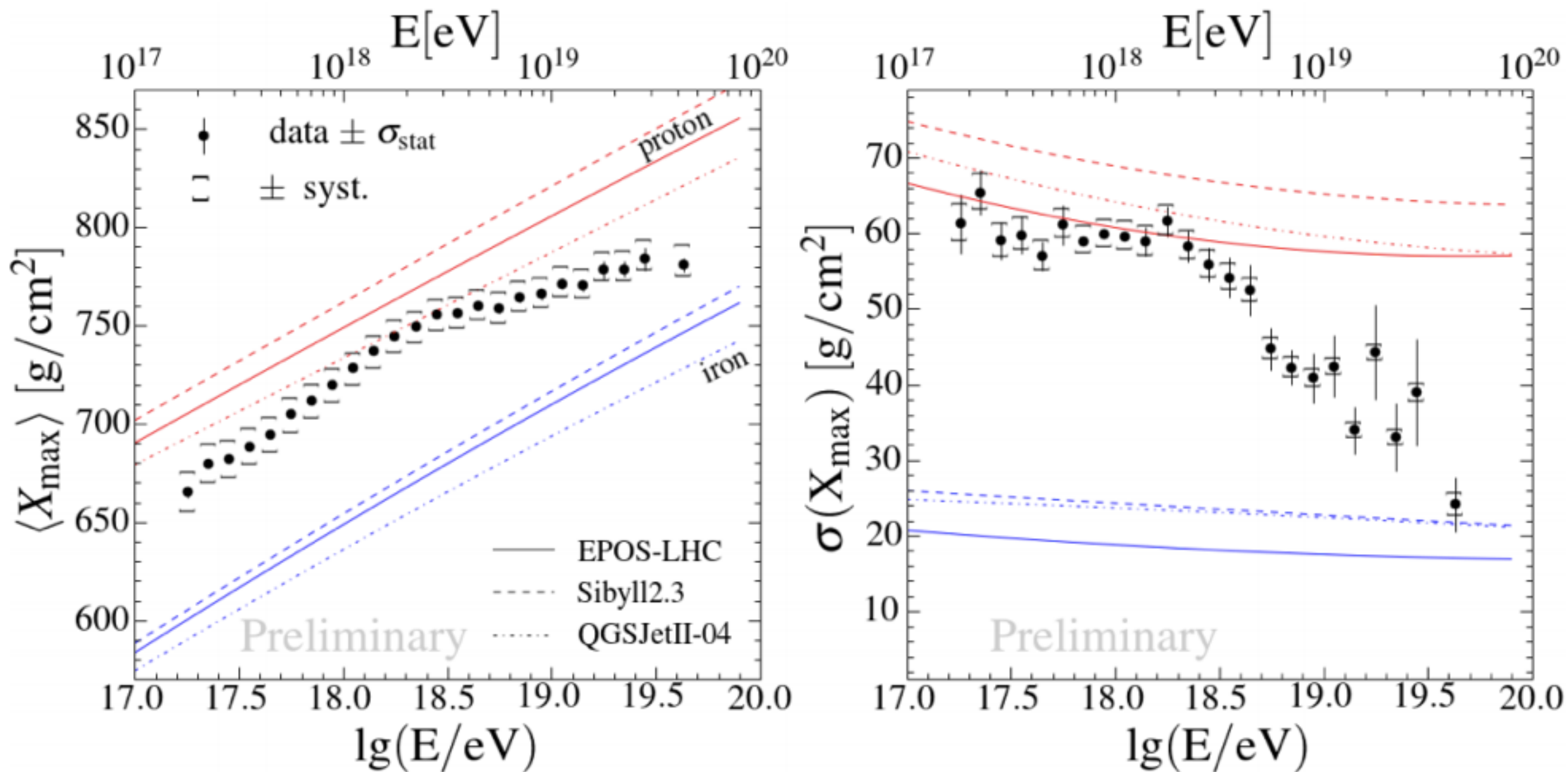
**SD-1500 inclined**  
19602 events  
 $\log(E) > 18.5$   
Exposure: 15121  $\text{km}^2 \text{ sr yr}$   
(38% increase wrt 2015)

Flux uncertainty: 5%

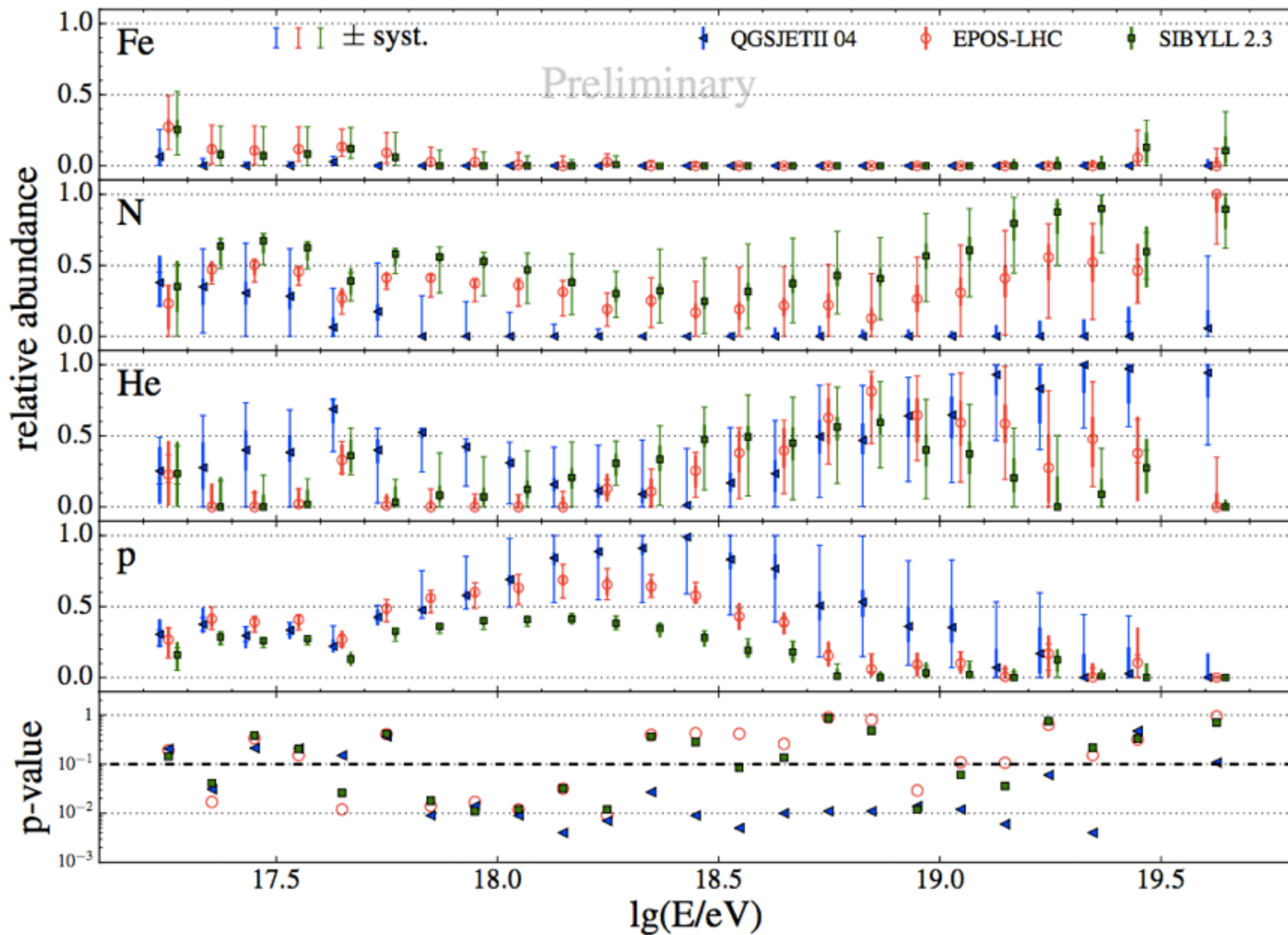
# Energy spectrum



# $X_{\max}$ moments



# $X_{\max}$ distributions



# Interpretation of spectrum and $X_{\max}$ data

---

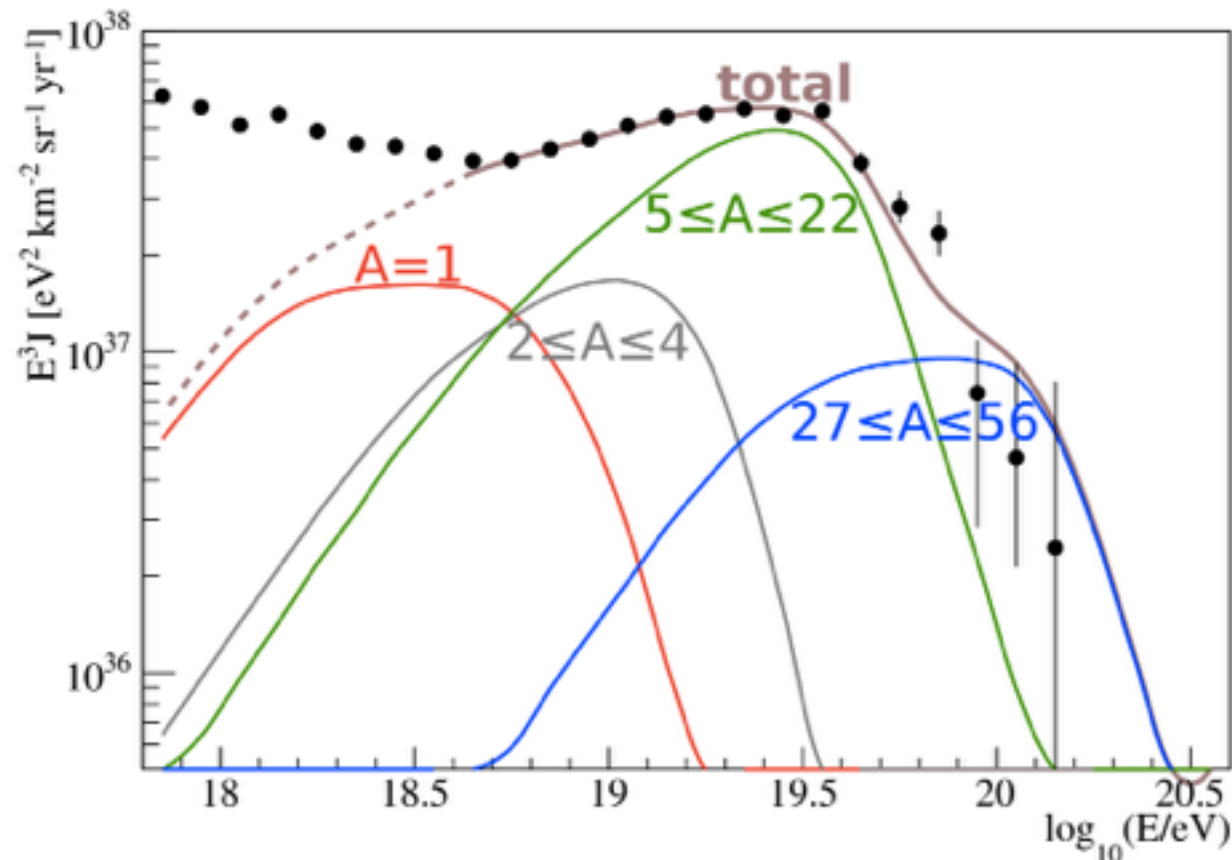
[Auger coll., JCAP 04(2017)038 — see also Aloisio, Berezhinsky & Blasi, JCAP 1410(2014)10]

- ◆ The  $X_{\max}$  measurements suggest a scenario with a **rigidity-dependent** maximum acceleration energy at the sources
  - ➔ Fit  $> 10^{18.7}$  eV both the energy spectrum and the  $X_{\max}$  measurements following a simple astrophysical scenario:
    - Identical sources homogeneously distributed in a comoving volume
    - Injection consisting only of  $^1\text{H}$ ,  $^4\text{He}$ ,  $^{14}\text{N}$ ,  $^{56}\text{Fe}$  (approximately equally spaced in  $\ln A$ )
    - Power-law spectrum at the sources with rigidity-dependent broken exponential cutoff:

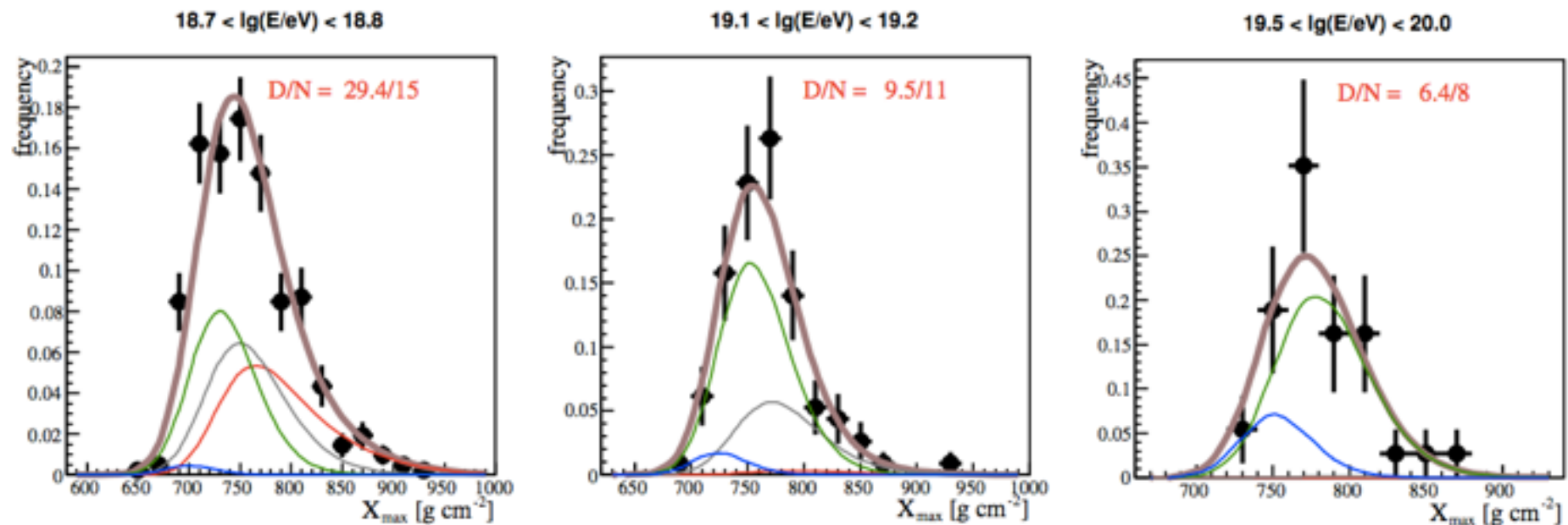
$$\frac{dN_{\text{inj},i}}{dE} = \begin{cases} J_0 p_i \left(\frac{E}{E_0}\right)^{-\gamma}, & E/Z_i < R_{\text{cut}} \\ J_0 p_i \left(\frac{E}{E_0}\right)^{-\gamma} \exp\left(1 - \frac{E}{Z_i R_{\text{cut}}}\right), & E/Z_i > R_{\text{cut}} \end{cases}$$

➔ 6 free parameters:  $(J_0, \gamma, R_{\text{cut}}, p_{\text{H}}, p_{\text{He}}, p_{\text{N}})$ ;  $p_{\text{Fe}} = 1 - p_{\text{H}} - p_{\text{He}} - p_{\text{N}}$

# Energy Loss vs Max. Acceleration Energy



- ➔ Hard spectral index, meal-rich injection, low cutoff ( $R_{\text{cut}} \sim 10^{18.7}$  V)
- Mainly due to narrow  $X_{\text{max}}$  distributions (little mixing of different masses at the same energy)
- **NB: Relies on extrapolations of the mass at UHE**



- red:  $A = 1$
- gray:  $2 \leq A \leq 4$
- green:  $5 \leq A \leq 22$
- blue:  $A \geq 23$
- thick brown: total
- black dots: Auger data

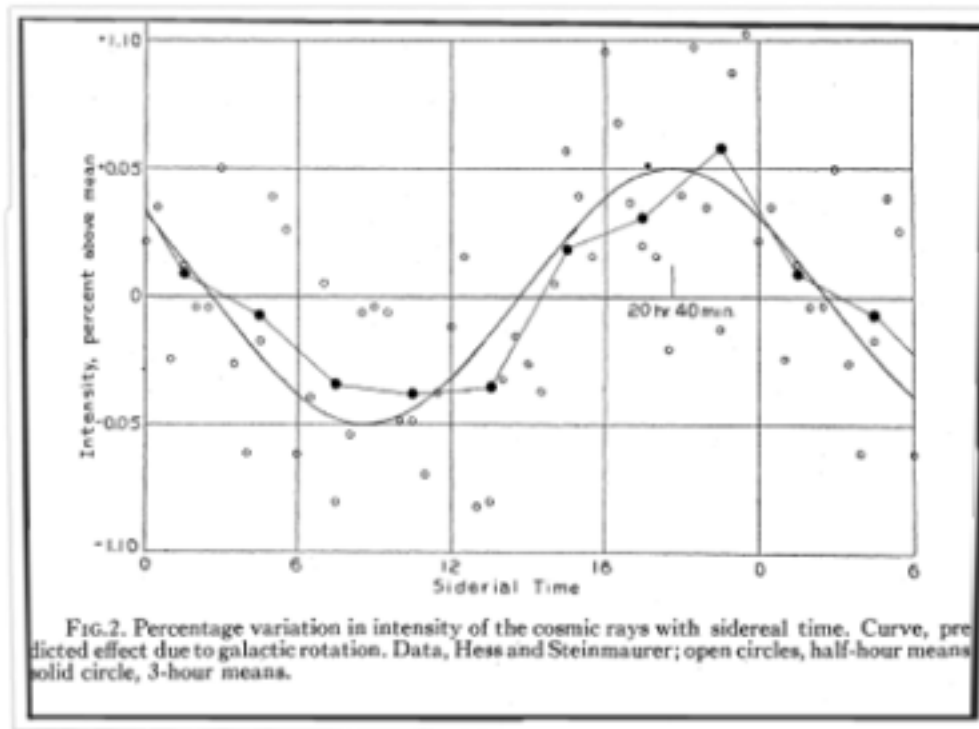
***iv*) Extragalactic pattern of cosmic-ray arrival directions  
above  $8 \times 10^{18}$  eV**

# All extragalactic?

THE  
PHYSICAL REVIEW  
*A Journal of Experimental and Theoretical Physics*  
VOL. 47, No. 11      JUNE 1, 1935      SECOND SERIES

## An Apparent Effect of Galactic Rotation on the Intensity of Cosmic Rays

ARTHUR H. COMPTON, *University of Chicago and Oxford University* AND IVAN A. GETTING, *Oxford University*  
(Received April 12, 1935)



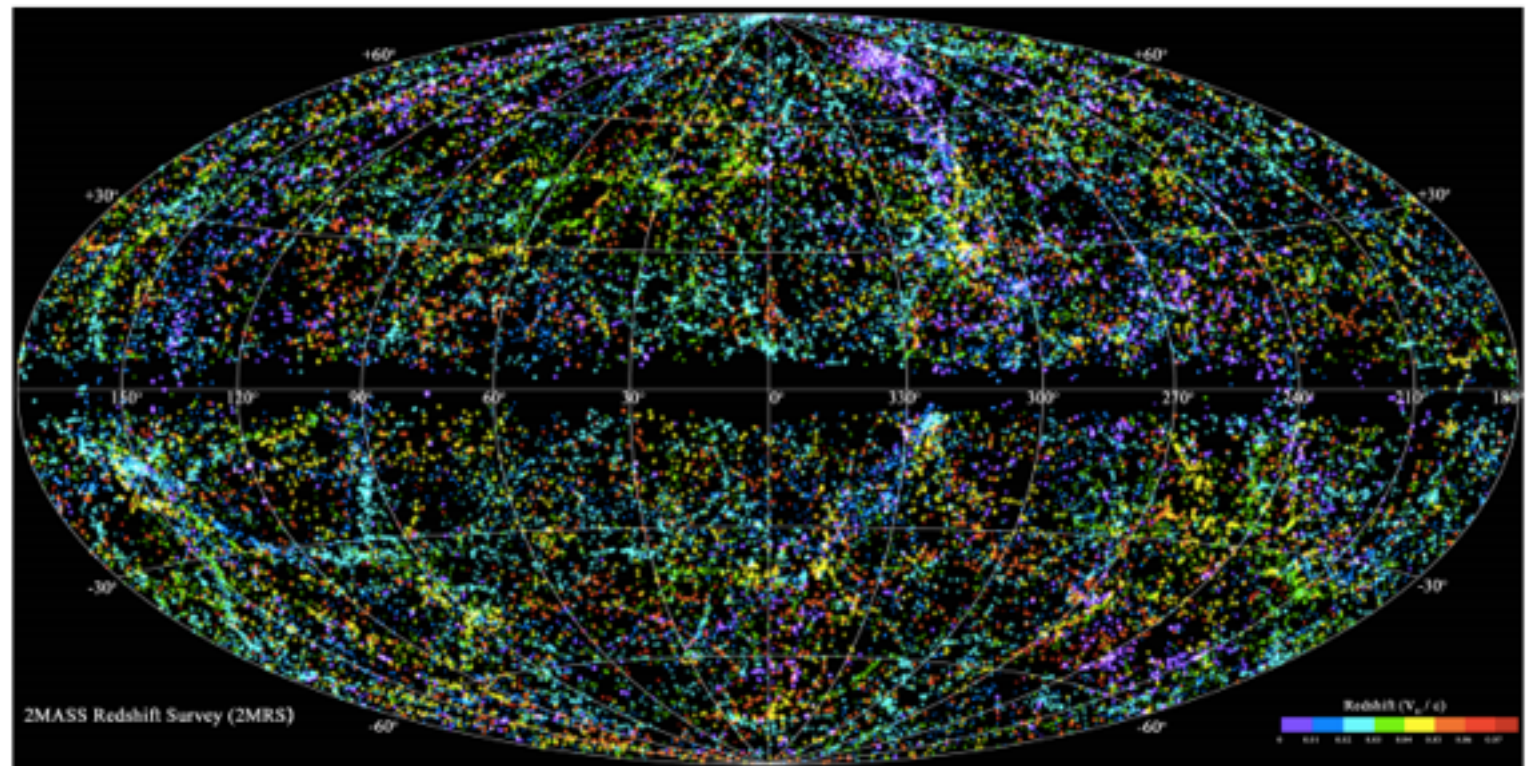
While we must await some such measurements before we can consider the effect due to the rotation of the galaxy as established, the quantitative agreement with the predictions as shown in Fig. 2 gives a strong presumption in its favor. Its existence would imply that an important part of the cosmic rays originates outside of our galaxy. If its magnitude is found to be as great as we have predicted, it will imply that practically all the cosmic radiation has an extragalactic origin.

# Large-scale anisotropies

---

- Galactic origin: strong anisotropies suggestive of the Milky way structure
- Extragalactic origin: inhomogeneous large-scale distribution of nearby sources
- Many dependences: source distribution, CR composition, nearby dominating sources, magnetic fields...

2MASS redshift survey



# Harmonic analysis

---

## ► Weighted harmonic analysis

$$a^x = \frac{2}{\mathcal{N}} \sum_{i=1}^N w_i \cos x_i, \quad b^x = \frac{2}{\mathcal{N}} \sum_{i=1}^N w_i \sin x_i$$

$\alpha$ : right ascension

$\phi$ : azimuth

$$\mathbf{x} = \alpha \text{ or } \phi \quad \mathcal{N} = \sum_{i=1}^N w_i$$

weights  $\longrightarrow$  small variations in coverage and tilt of the array

[ApJ suppl. 203 (2012) 34]

$$r^\alpha = \sqrt{(a^\alpha)^2 + (b^\alpha)^2}, \quad \varphi^\alpha = \text{atan} \frac{b^\alpha}{a^\alpha}$$

Amplitude and phase of the first harmonic modulation

► p.d.f. for amplitude/phase known for isotropy/anisotropy [Linsley, 1975]

# Control of the event rate

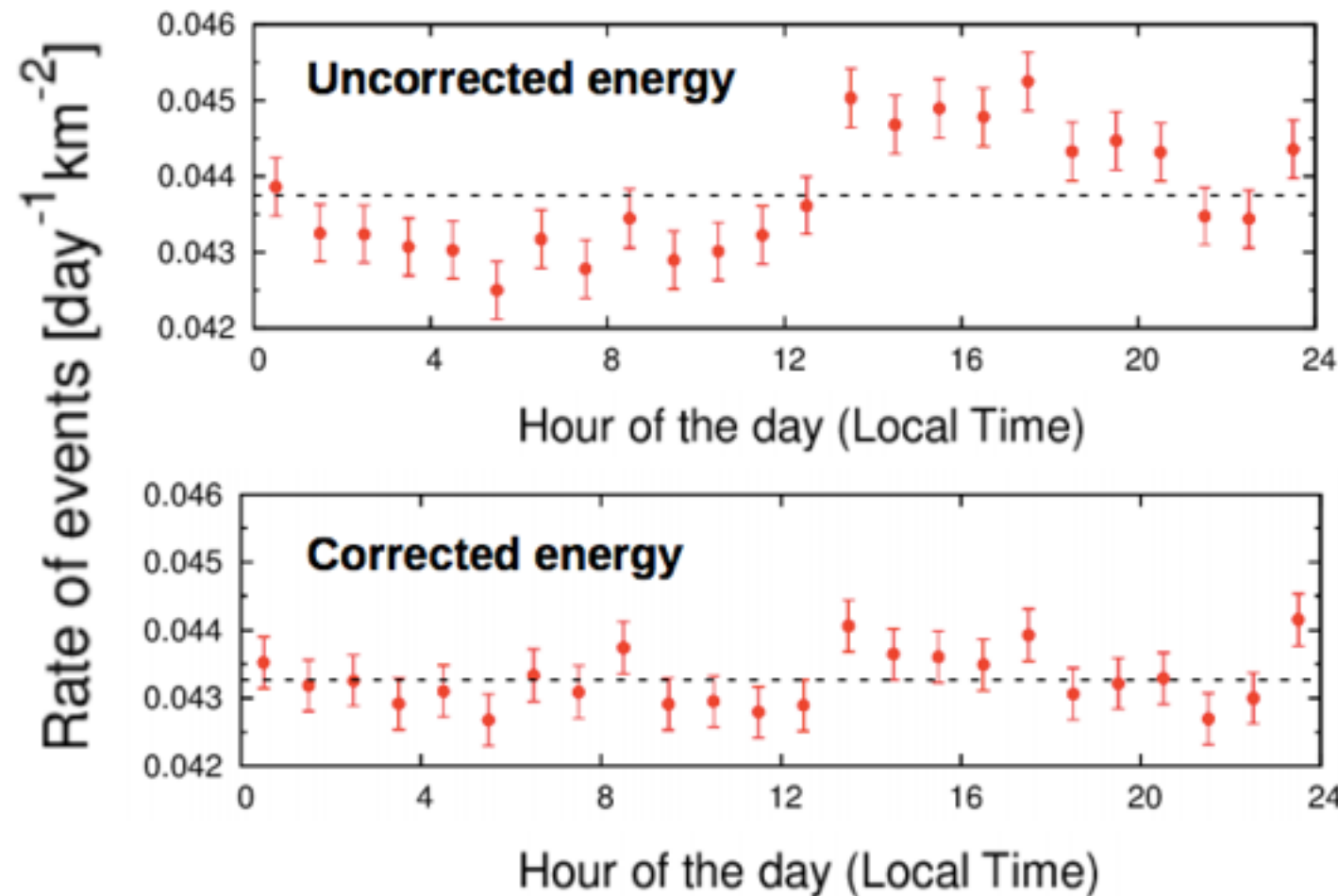
## ► Energies corrected by atmospheric changes for $\theta < 60^\circ$

- Air-density → lateral distribution of EM component
- Pressure → longitudinal depth of observation



Induces modulations of  $\pm 1.7\%$  in solar frequency

[Auger Coll. JINST 12 (2017) P02006]



Negligible effects at  $60^\circ < \theta < 80^\circ$   
(EM component suppressed)

## ► Geomagnetic field breaks circular symmetry of showers

Effect accounted in energy estimation

azimuth spurious modulation  $\sim 0.7\%$

[Auger Coll. JCAP 11 (2011) 022]

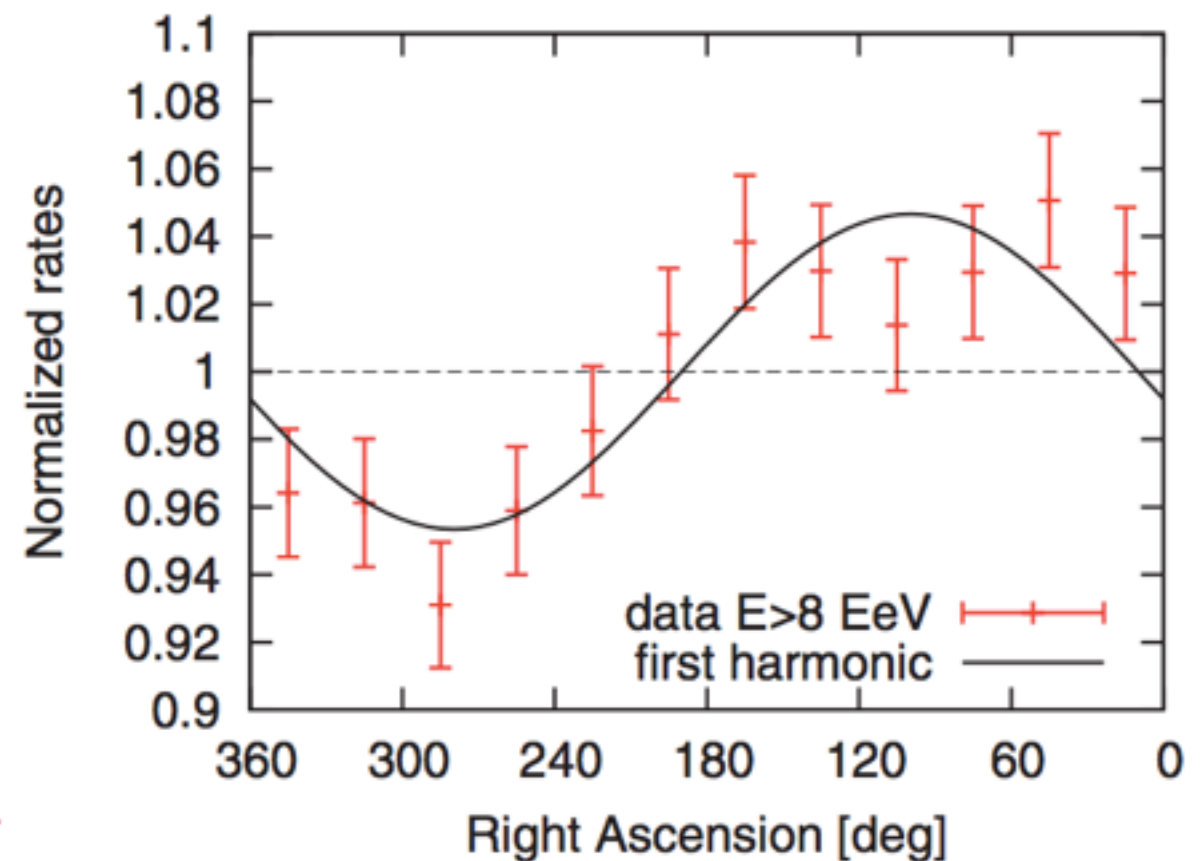
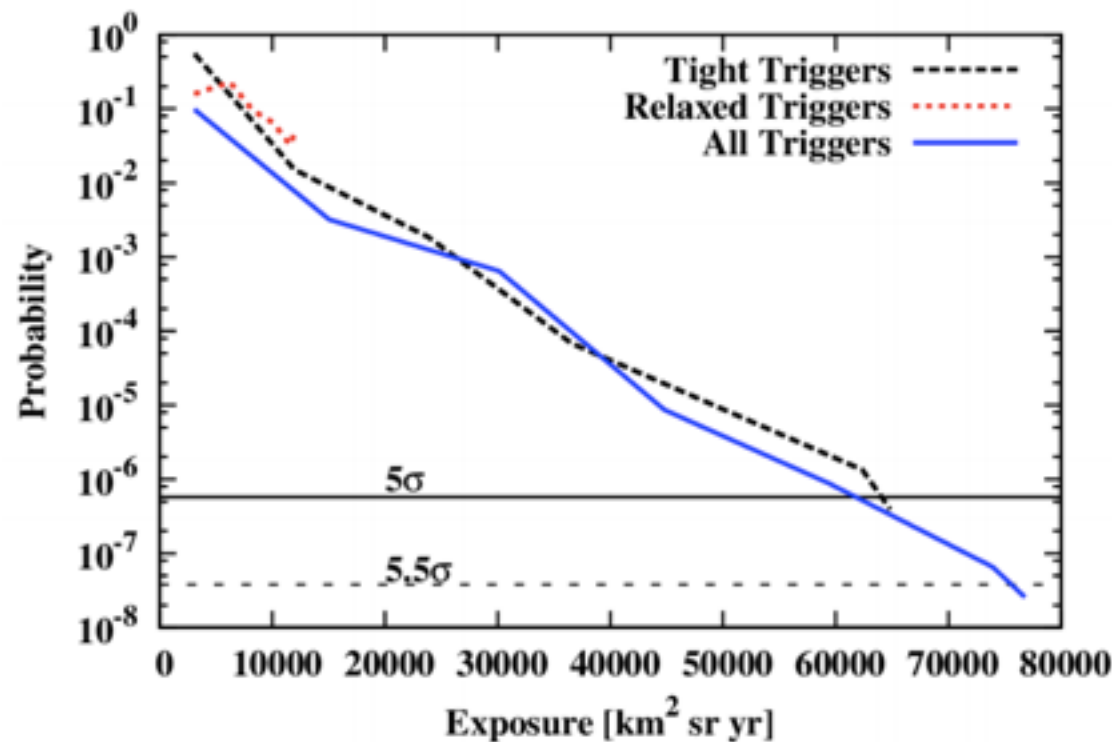
# First harmonic in right ascension

$E$ [EeV]	$N$	$a^\alpha$	$b^\alpha$	$r^\alpha$	$\varphi^\alpha$ [°]	$P(\geq r^\alpha)$
4 - 8	81 701	$0.001 \pm 0.005$	$0.005 \pm 0.005$	$0.005^{+0.006}_{-0.002}$	$80 \pm 60$	0.60
$\geq 8$	32 187	$-0.008 \pm 0.008$	$0.046 \pm 0.008$	$0.047^{+0.008}_{-0.007}$	$100 \pm 10$	$2.6 \times 10^{-8}$

**Table 1:** Results of the first harmonic analysis in right ascension.

[4 – 8] EeV: compatible with isotropy  $\rightarrow r^\alpha < 0.012$  @ 95% CL

$E > 8$  EeV: significant modulation @  $5.6\sigma$   $\rightarrow$   $p$ -value  $\sim 20$  times smaller than the  $5\sigma$  discovery limit<sup>1</sup>

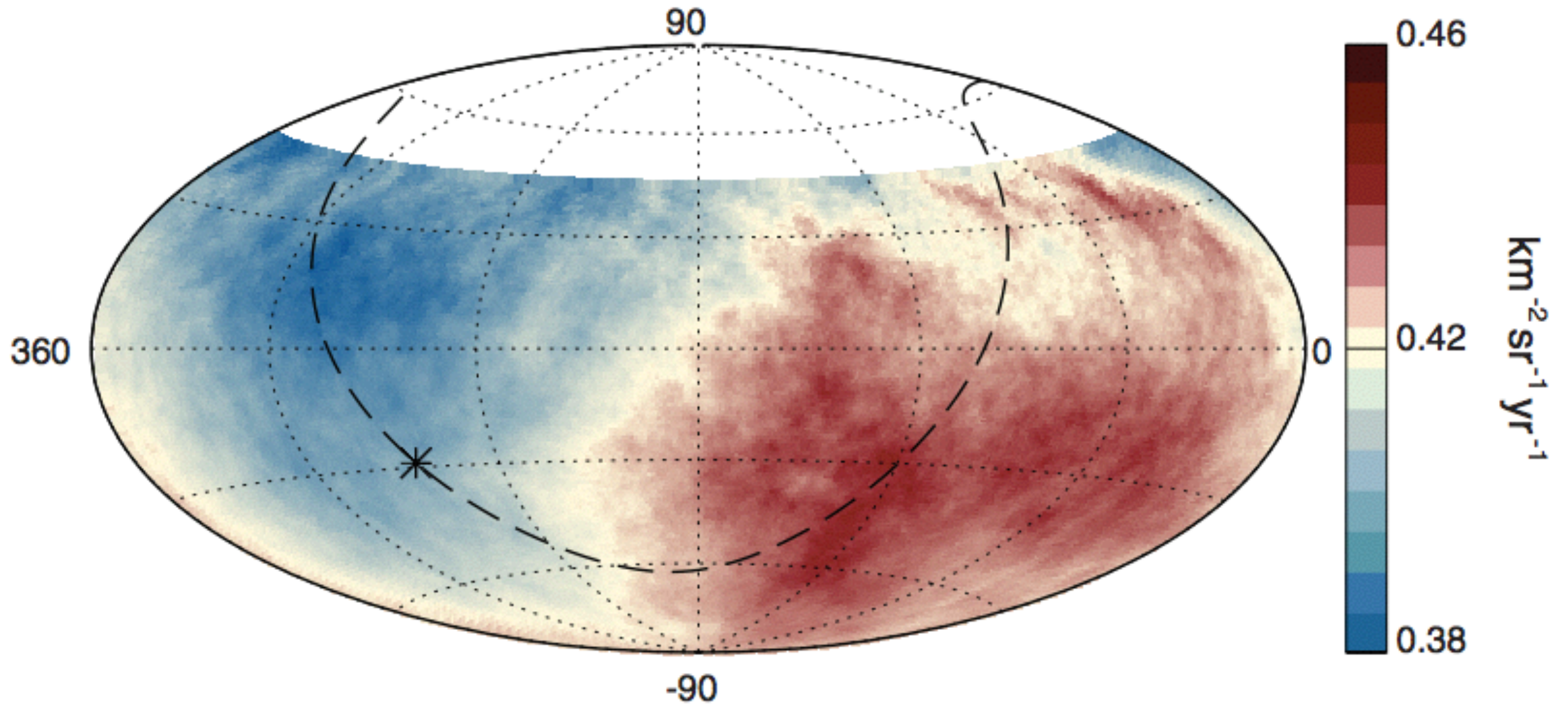


<sup>1</sup>penalizing for the energy bins explored  $\rightarrow$  significance above  $5.2\sigma$

# Flux pattern on the sphere

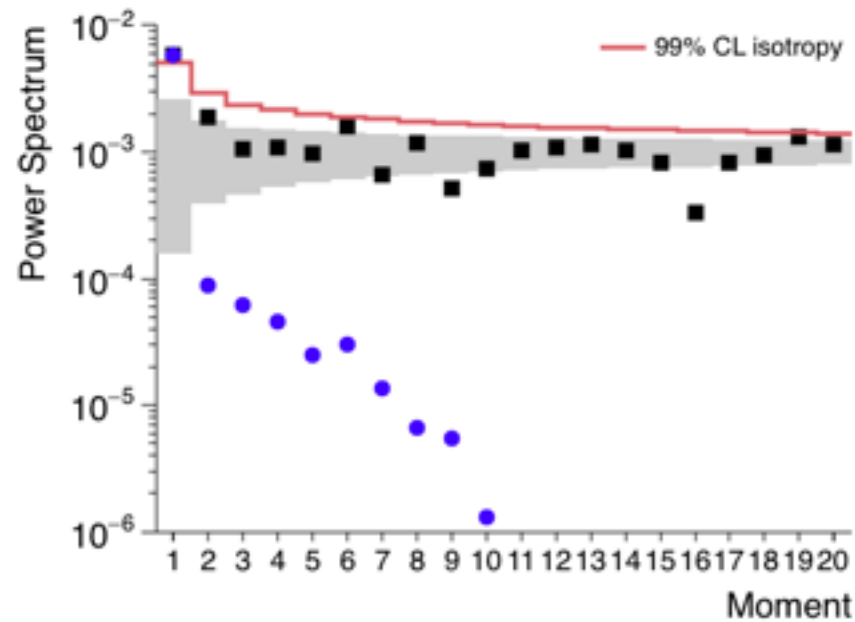
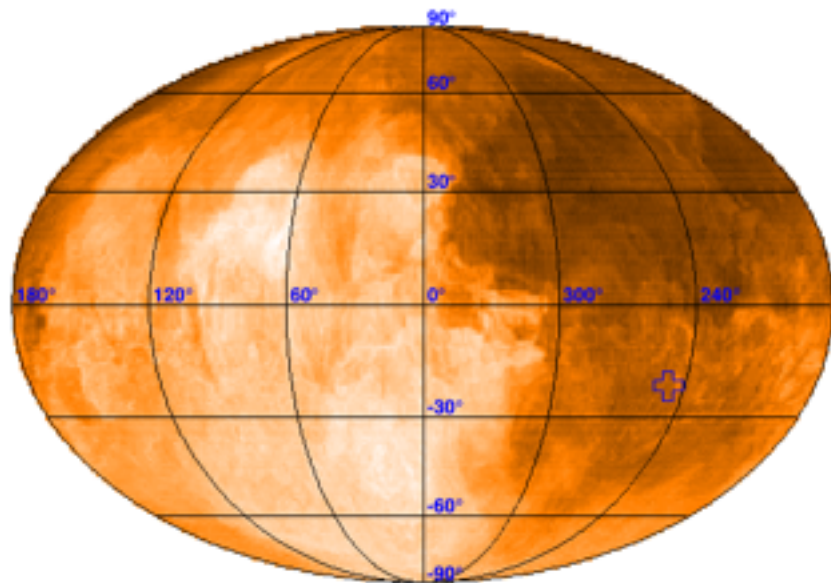
---

equatorial coordinates

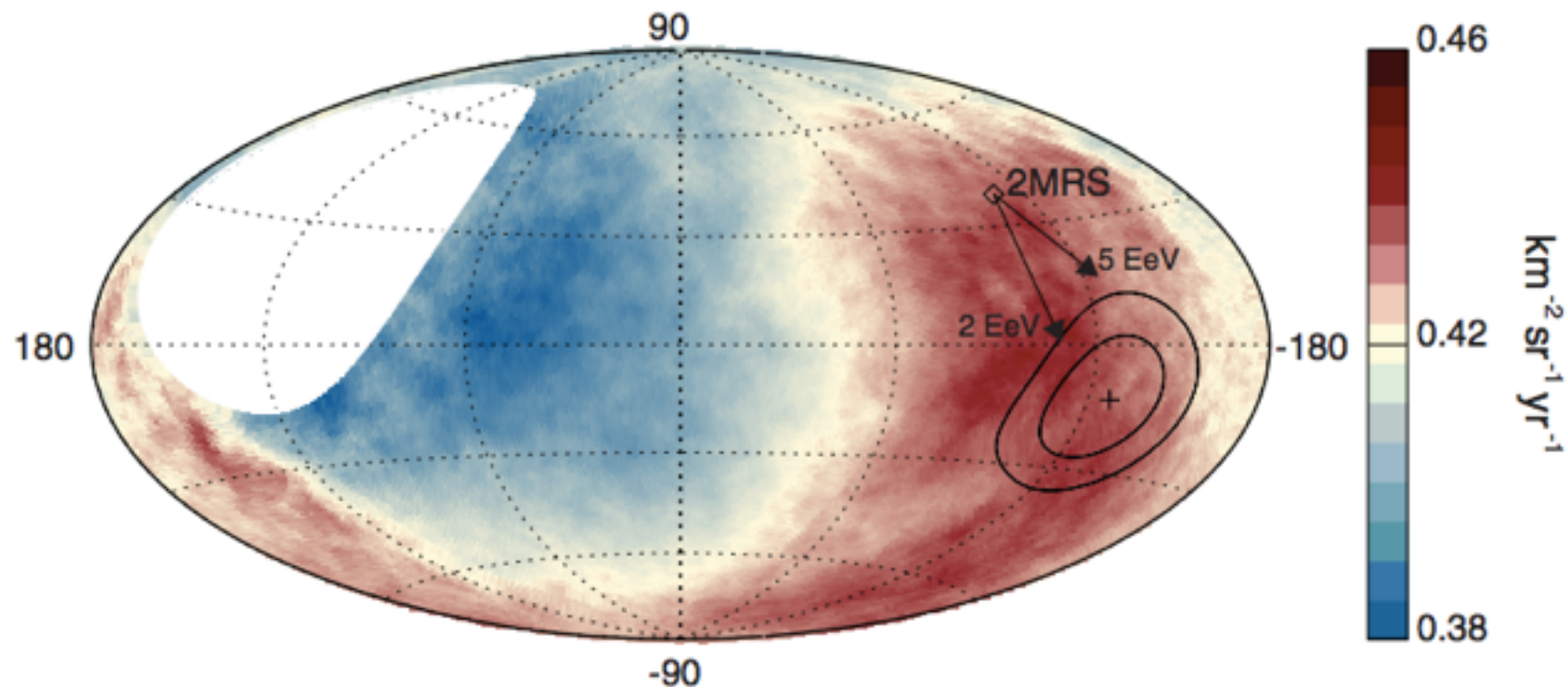


# Observational evidence of extragalactic UHECRs

Benchmark-scenario: Dipole at the entrance of the Galaxy



- ▶ Dipole not ‘destroyed’ by the GMF (JF12 model here)
- ▶ Detection of higher orders: probe of the extragalactic CR density outside from the Galaxy



Accounting GMF deflections

[Jansson and Farrar ApJ 757 (2012) 14]

$Z \sim 1.7 - 5$  at 10 EeV  $\rightarrow$   $E/Z \sim 2 - 5$  EeV

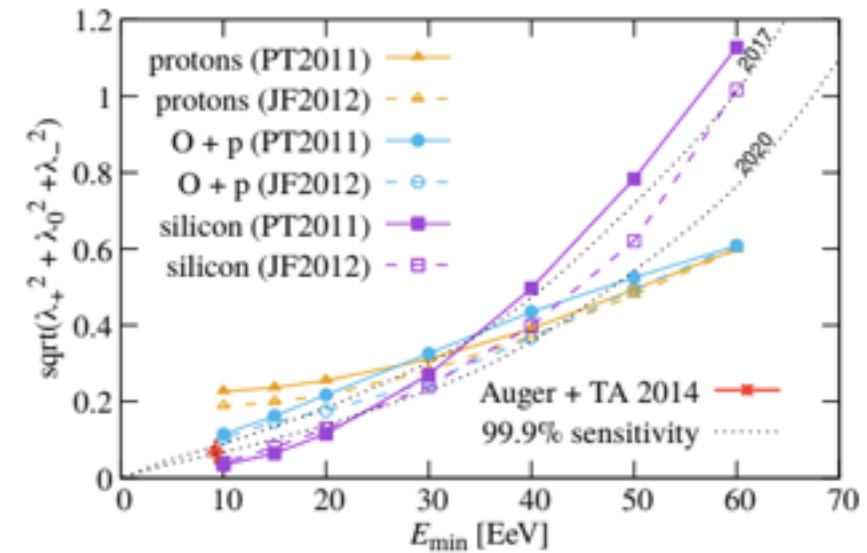
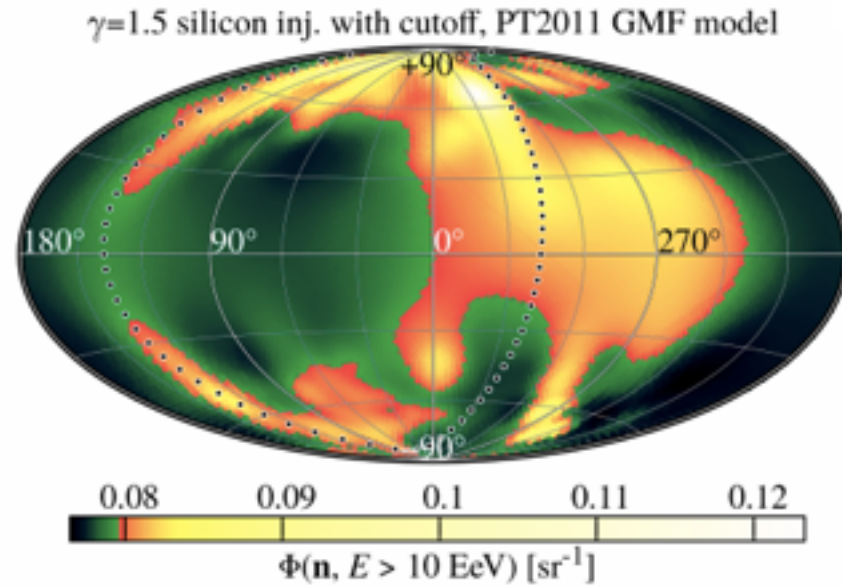
[Auger Coll. PRD 90 (2014) 122006]

# Flux pattern on the sphere

Higher order multipole signatures to constrain further models?

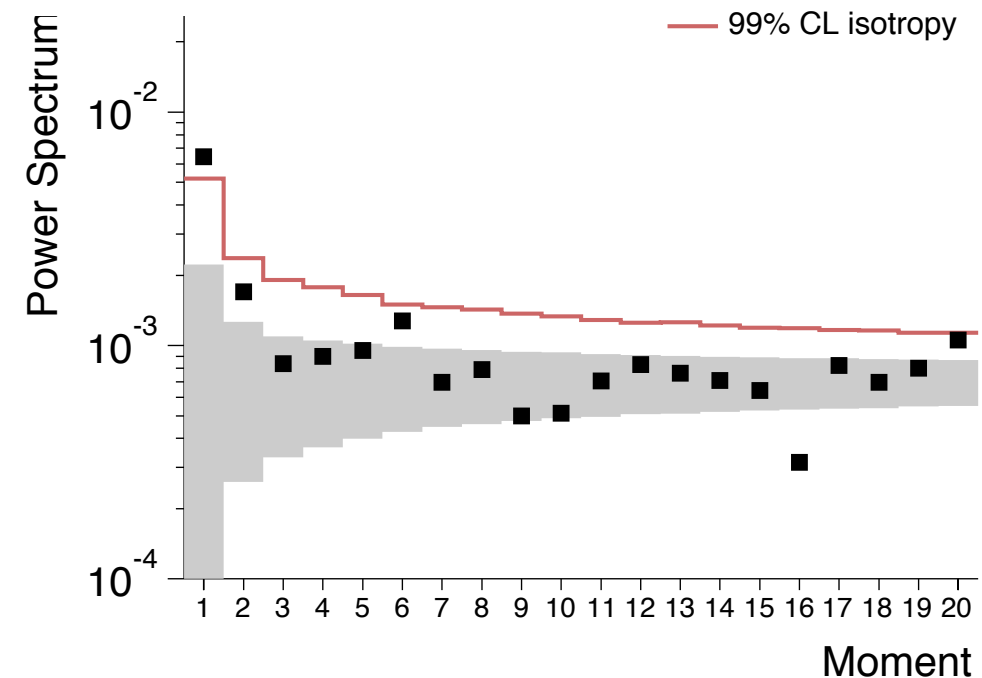
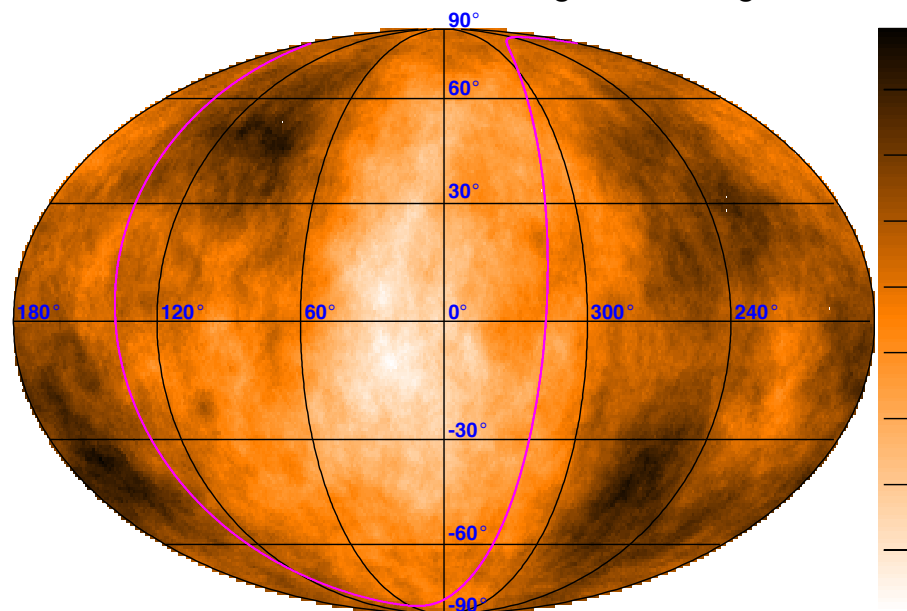
Requires full-sky coverage — joint Auger/TA analyses

[Di Matteo & Tyniakov, arXiv:1706.02534]



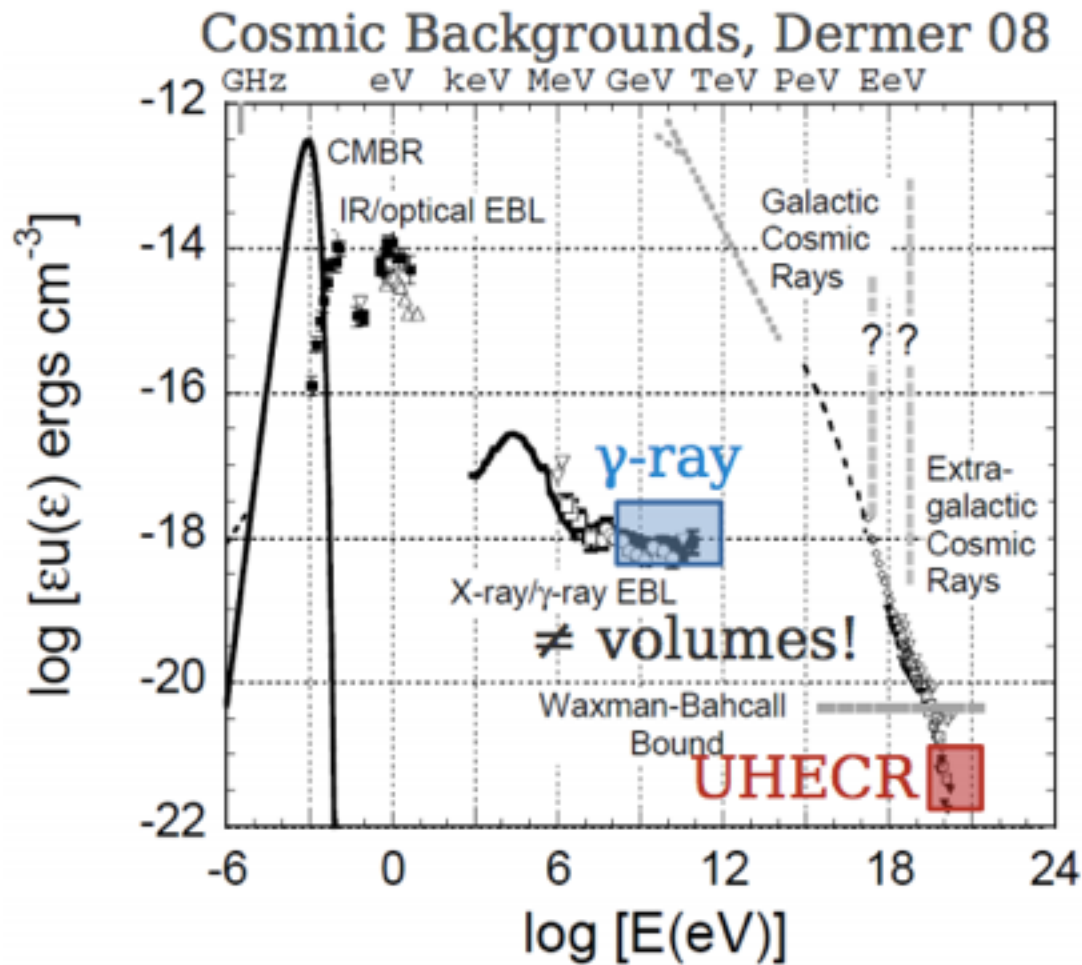
[Auger/TA coll., ICRC15]

Galactic Coordinates - 30 deg. smoothing

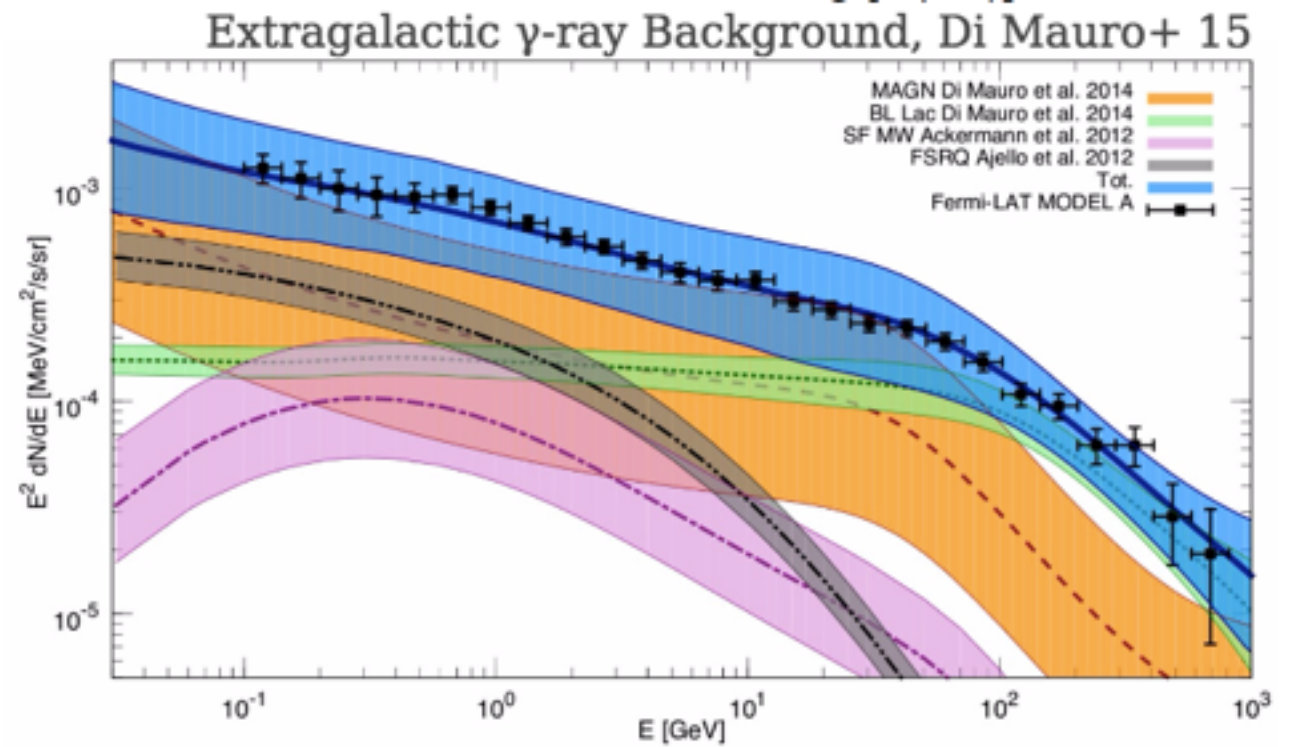


***v)* Correlation of UHECR arrival directions with the flux pattern of nearby star-forming galaxies**

# Extragalactic gamma-ray background

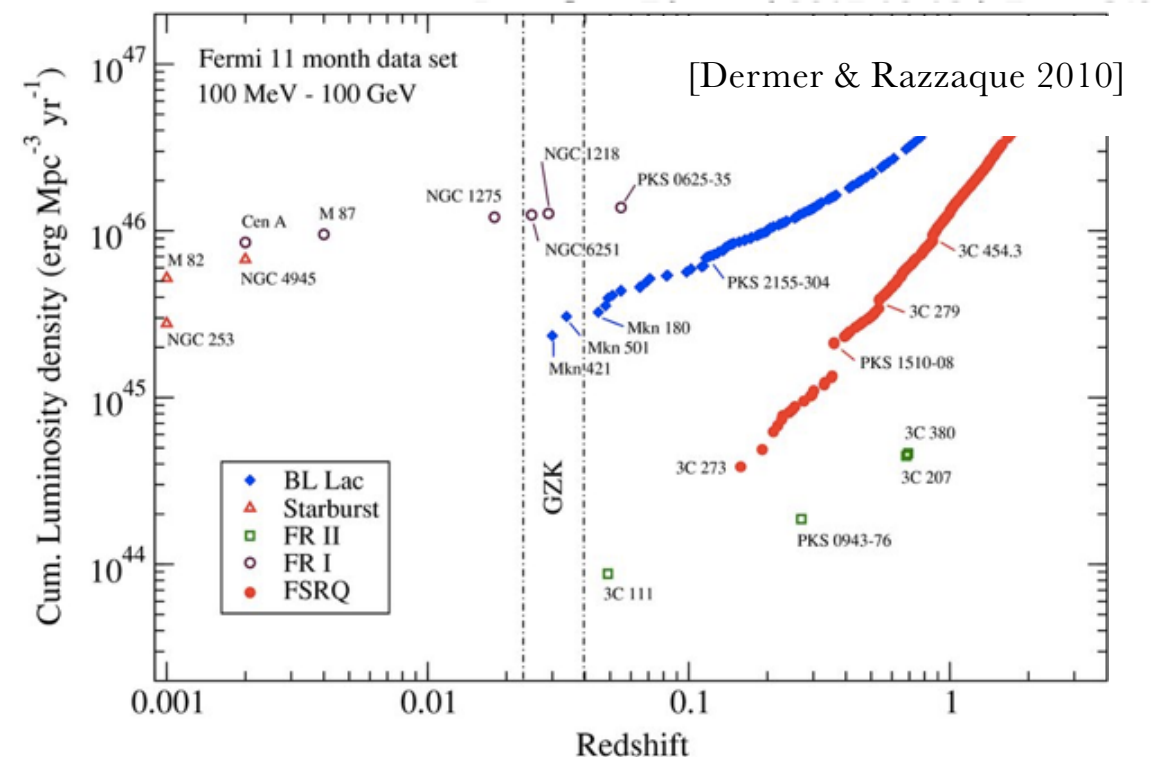


Extragalactic  $\gamma$ -ray background dominated by 2 types of sources:



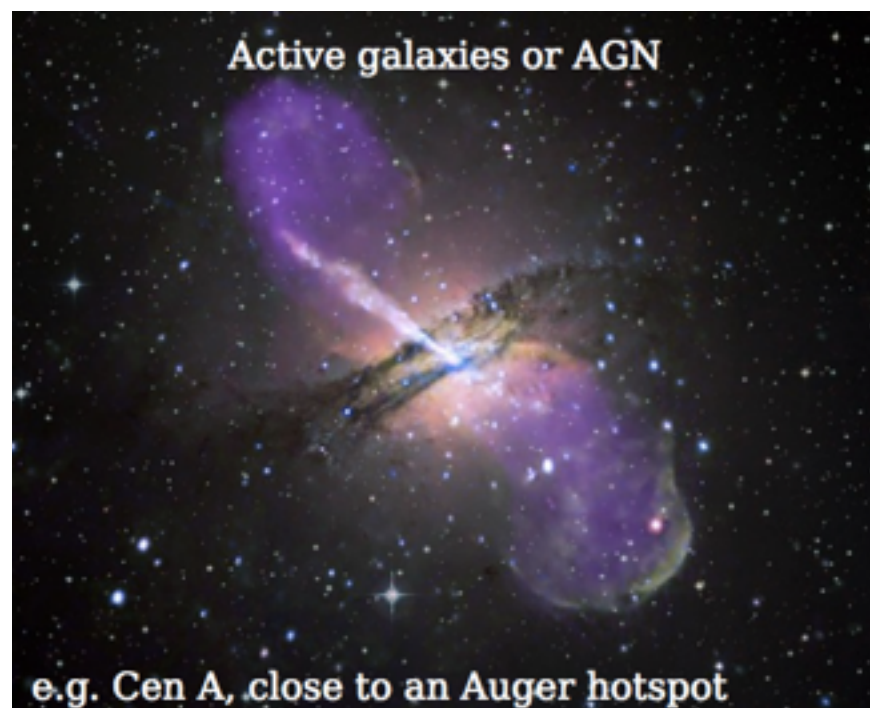
UHECR source candidates:  
requirement on power

- $>1$  EeV, energy production rate close to  $10^{45}$  erg  $\text{Mpc}^{-3} \text{yr}^{-1}$
- Both local SBGs & AGNs match this requirement



# Selection of *non-thermal* sources

---



Selected from the 2FHL catalog (*Fermi*-LAT,  $>50$  GeV), within 250 Mpc  
[Ackermann *et al.*, 2016]  
(leptonic processes preferred)

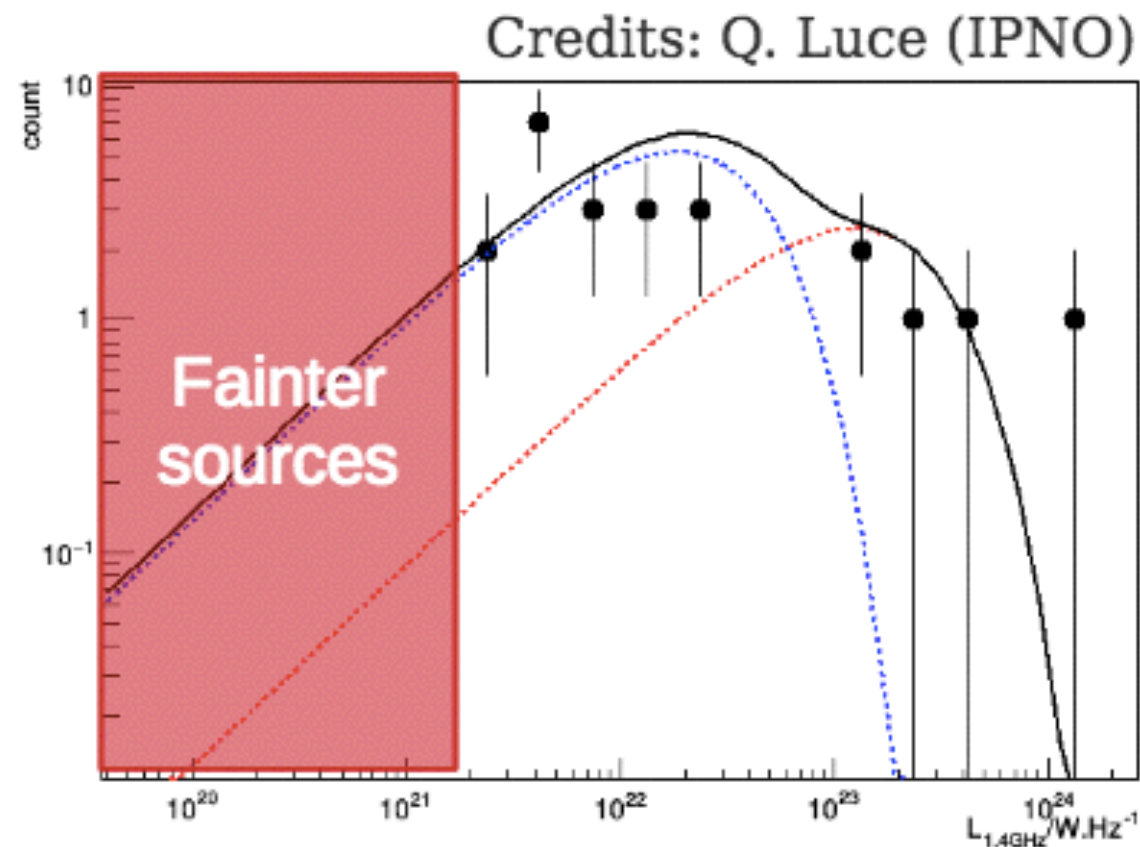
Selected from *Fermi*-LAT search list (HCN survey) within 250 Mpc, with radio flux  $>0.3$  Jy  
[Gao & Salomon, 2005]  
(hadronic processes preferred)

**Assumption:** UHECR flux  $\propto$  non-thermal photon flux

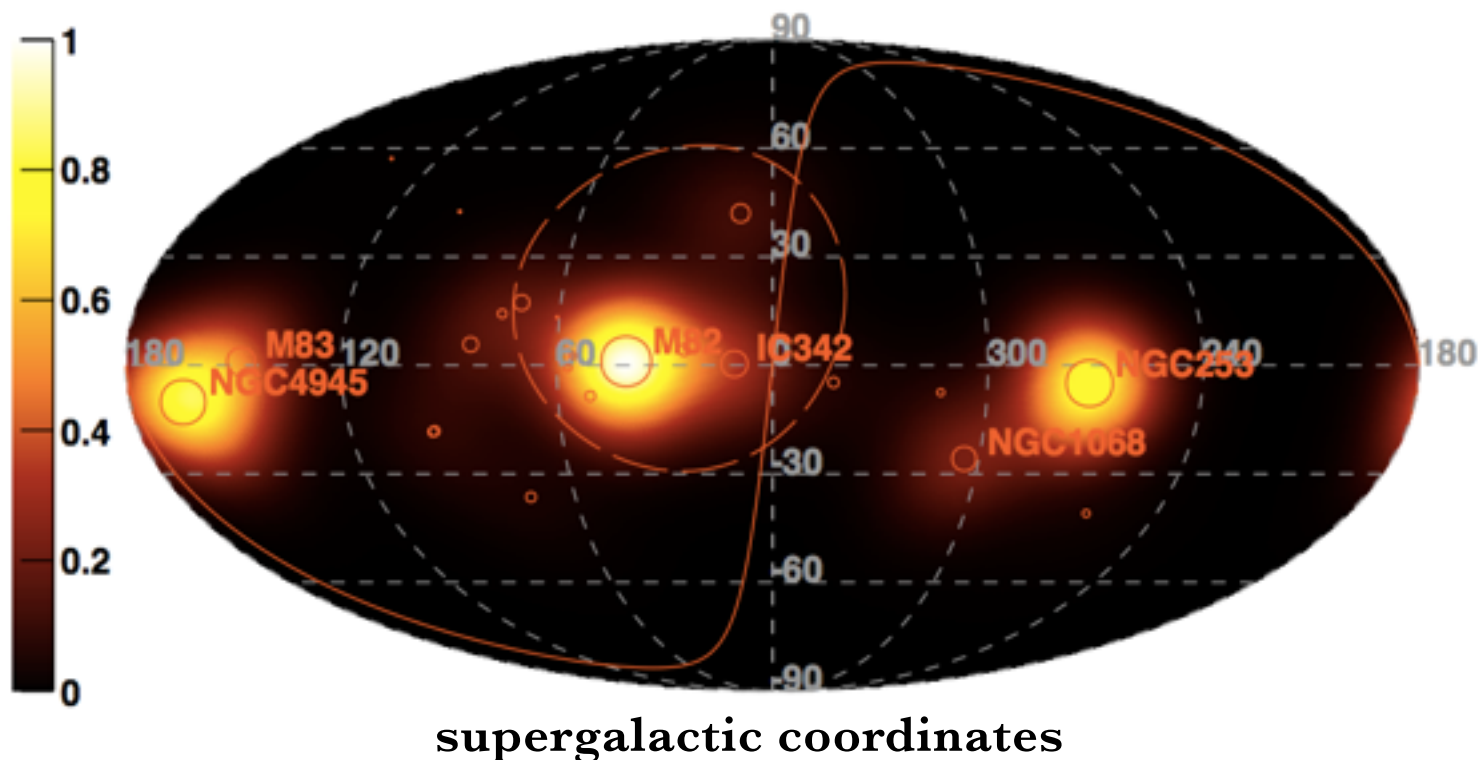
# Catalog of star-forming galaxies

## GeV—TeV observations

- **TeV:** M 82 (0.9% Crab), NGC 253 (0.2% Crab), NGC 4945  $\emptyset$ , NGC 1068 (<5%), M 83 (<2%)
  - **GeV:** M 82, NGC 253, NCG 4945, NGC 1068 firmly detected. GeV/FIR/radio correlation
- ➔ Flux at 1.4 GHz used as a **proxy** for the UHECR flux



Model Flux Map - Starburst galaxies -  $E > 39$  EeV

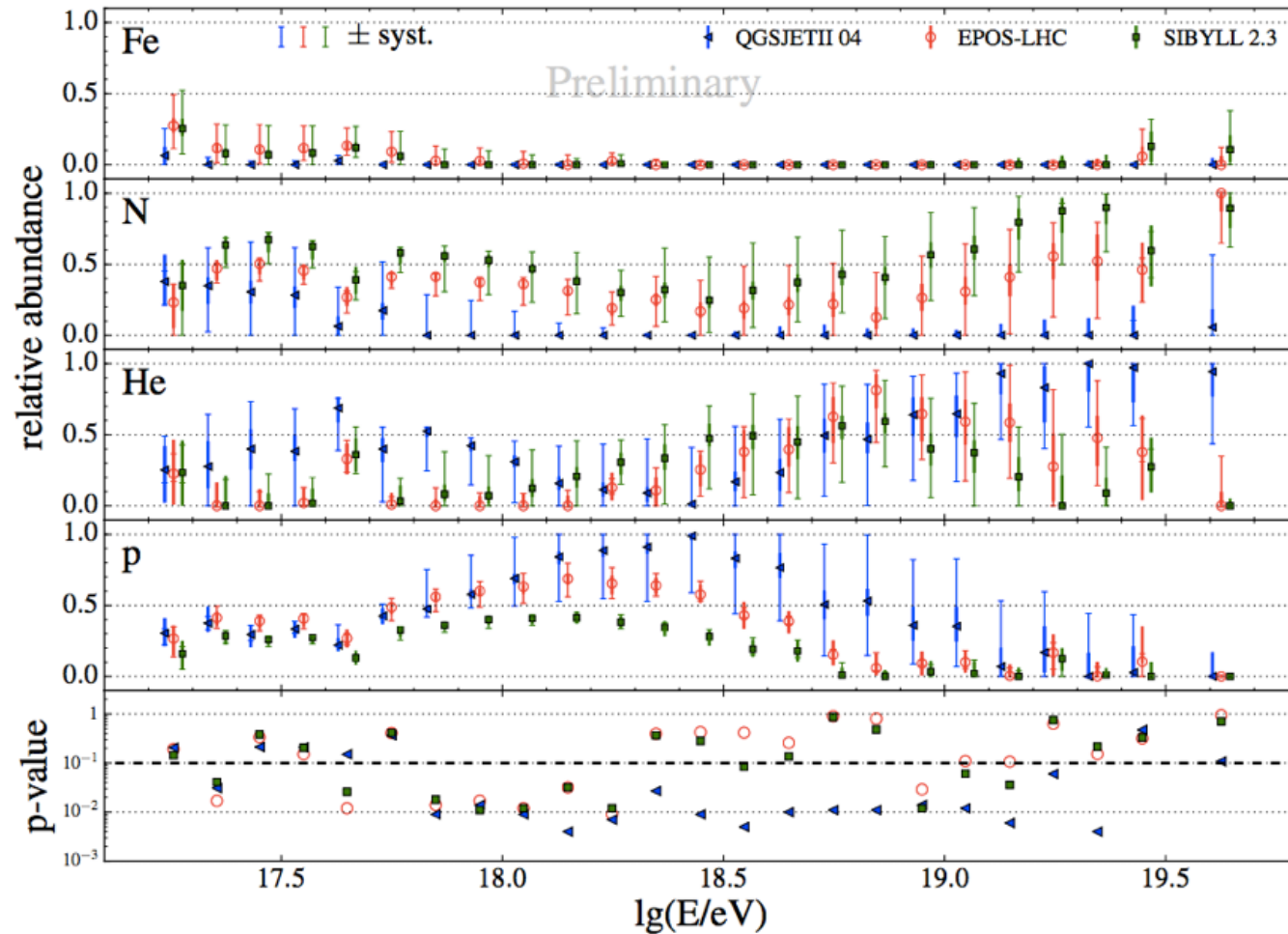


## Selected catalog

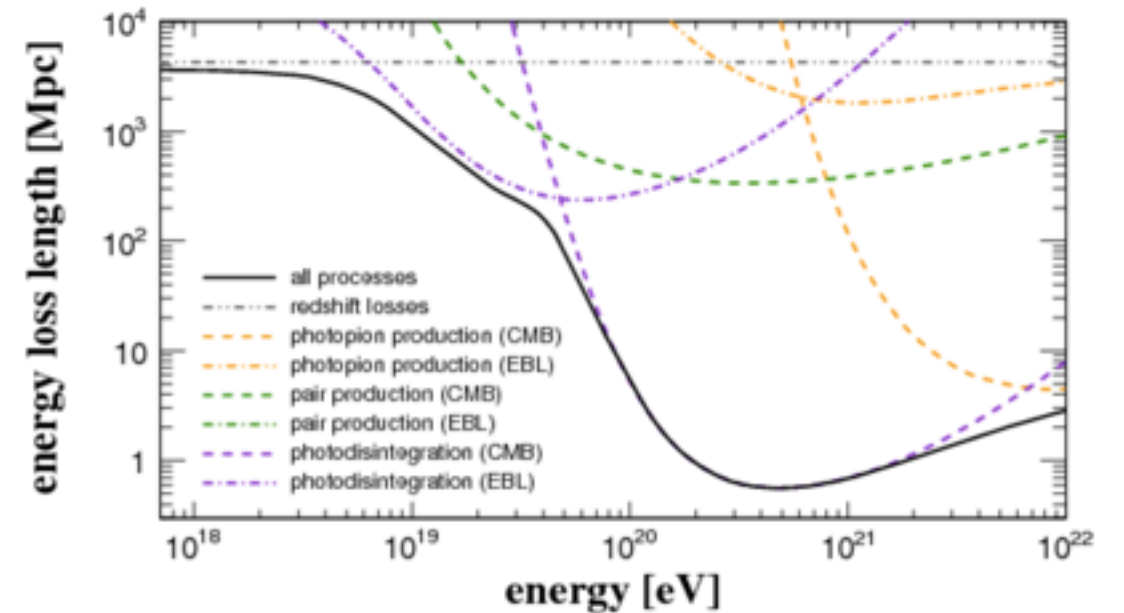
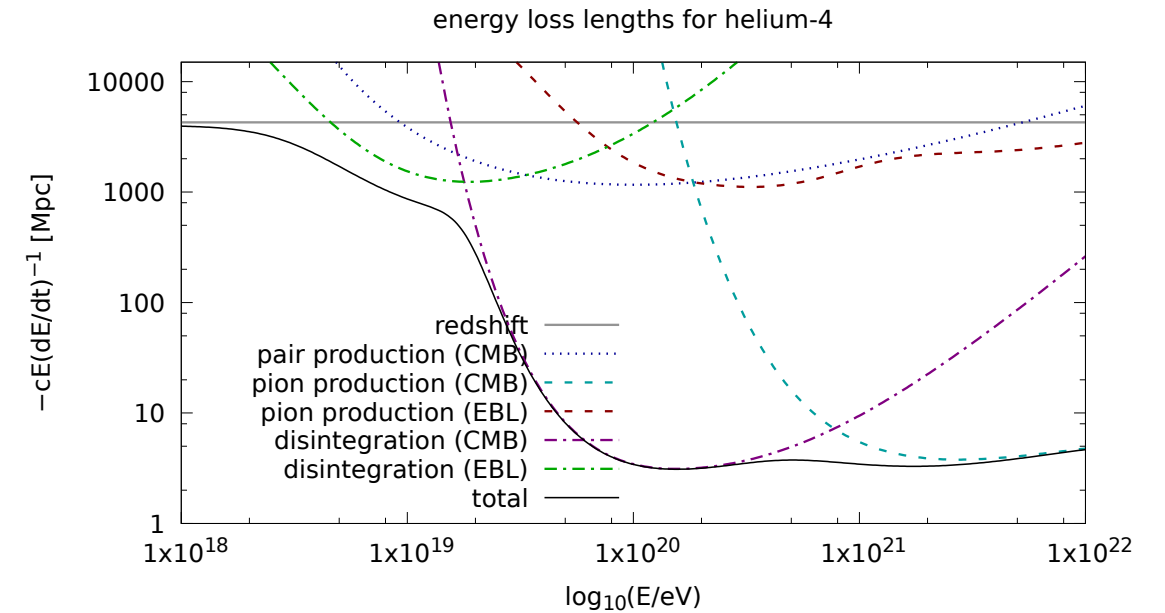
- ApJ 755, 164 (2012)
- Cut @ 0.3 Jy to maximize the completeness
- Cut that matches a  $\sim 200$  Mpc GZK horizon: take the most luminous source in the sample, place it as far away as you can to detect it above 0.3 Jy  $\rightarrow$  173 Mpc
- 23 brightest (/63) —  $\sim 80\%$  of total flux

# UHECR horizons

A mixture of He/CNO nuclei  
in the energy range of interest



[Alves Batista, Boncioli, Di Matteo et al., JCAP10(2015)063]



☞ Small horizons already @ 30-40 EeV

# Test statistics of alternative vs null

Luminosity distribution: **non-equal** sources,  
flux may be dominated by strong local sources

👉 Analysis method: test arrival directions vs **density maps**

*null*

$$L(-,0) = \prod_{\text{events}} [\text{exposure}] (\mathbf{n}_i)$$

*alternative*

$$L(\vartheta, \alpha) = \prod_{\text{events}} [\text{exposure} \times \text{model}(\vartheta, \alpha)] (\mathbf{n}_i)$$

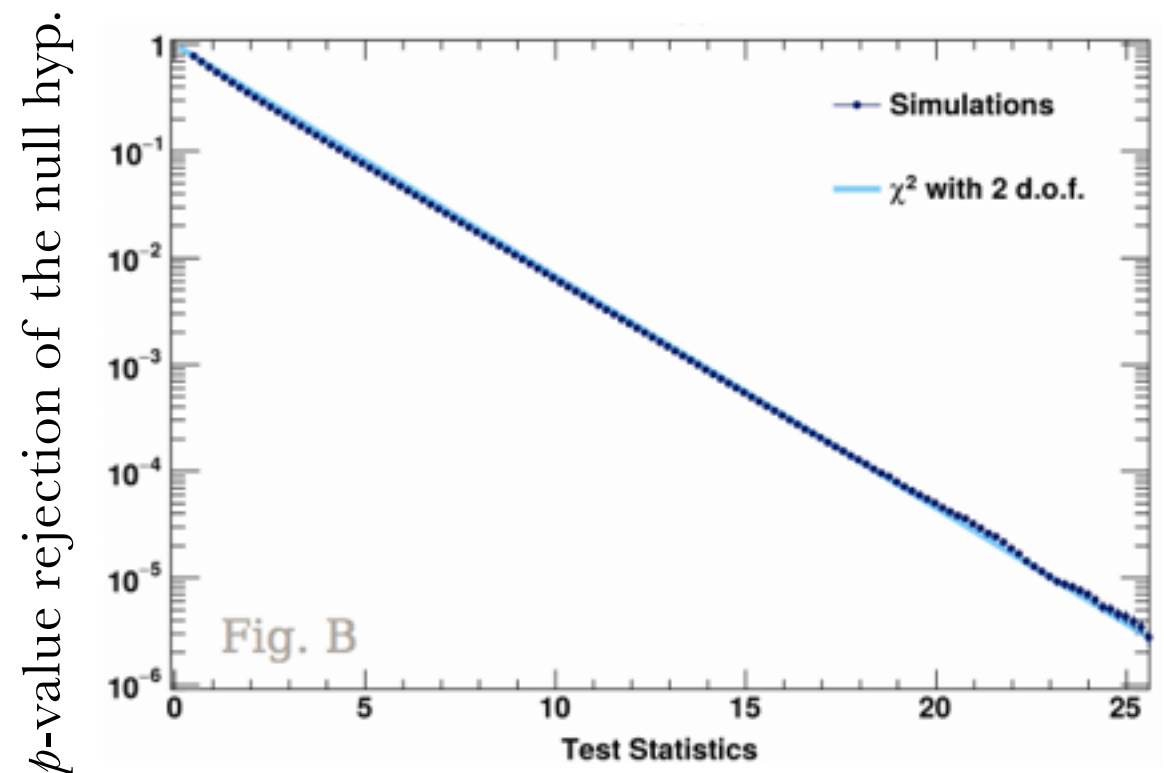
$\alpha$ : signal fraction

$\vartheta$ : search radius (no magnetic offset)

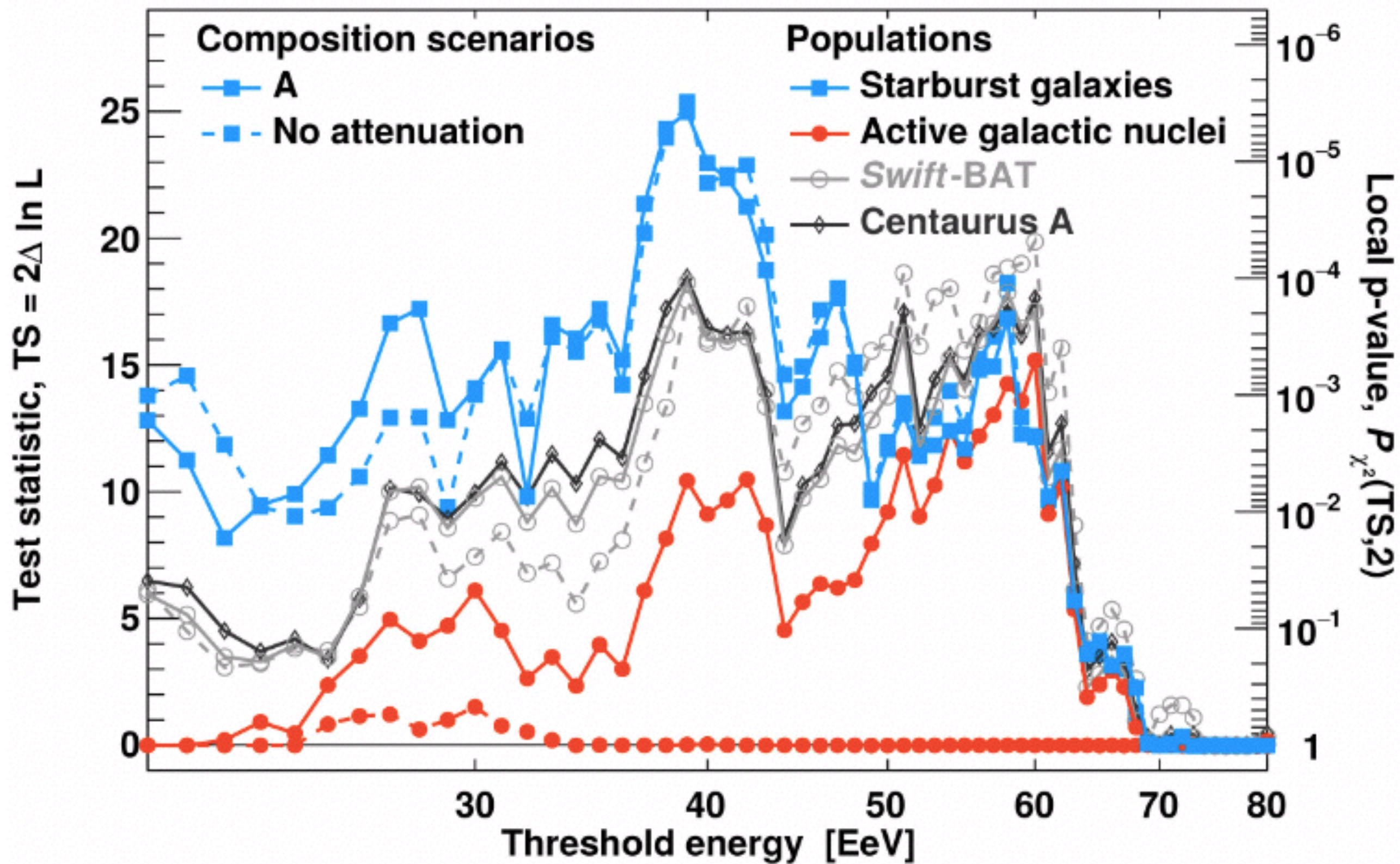
model:  $[\alpha \times \text{sources} + (1-\alpha) \times \text{isotropy}] \otimes \text{Gauss}(\vartheta)$

Test statistics (TS): likelihood ratio

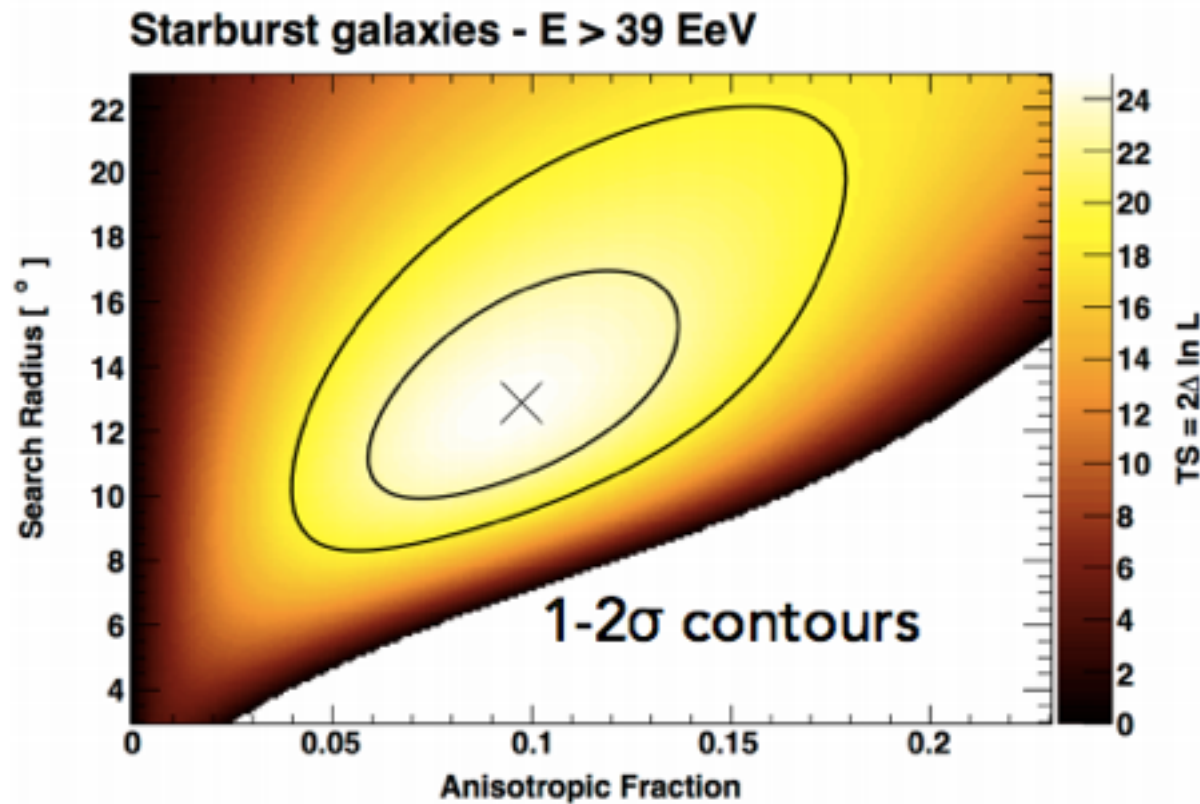
- $TS = 2 \ln(L(\vartheta, \alpha) / L(-, 0))$
- **Nested** hypotheses: TS is  $\chi^2$ -distributed with 2 d.o.f. (2 free parameters  $\vartheta, \alpha$ )



# Results: test statistics vs energy threshold



# Best fit parameters



## Starburst Galaxies

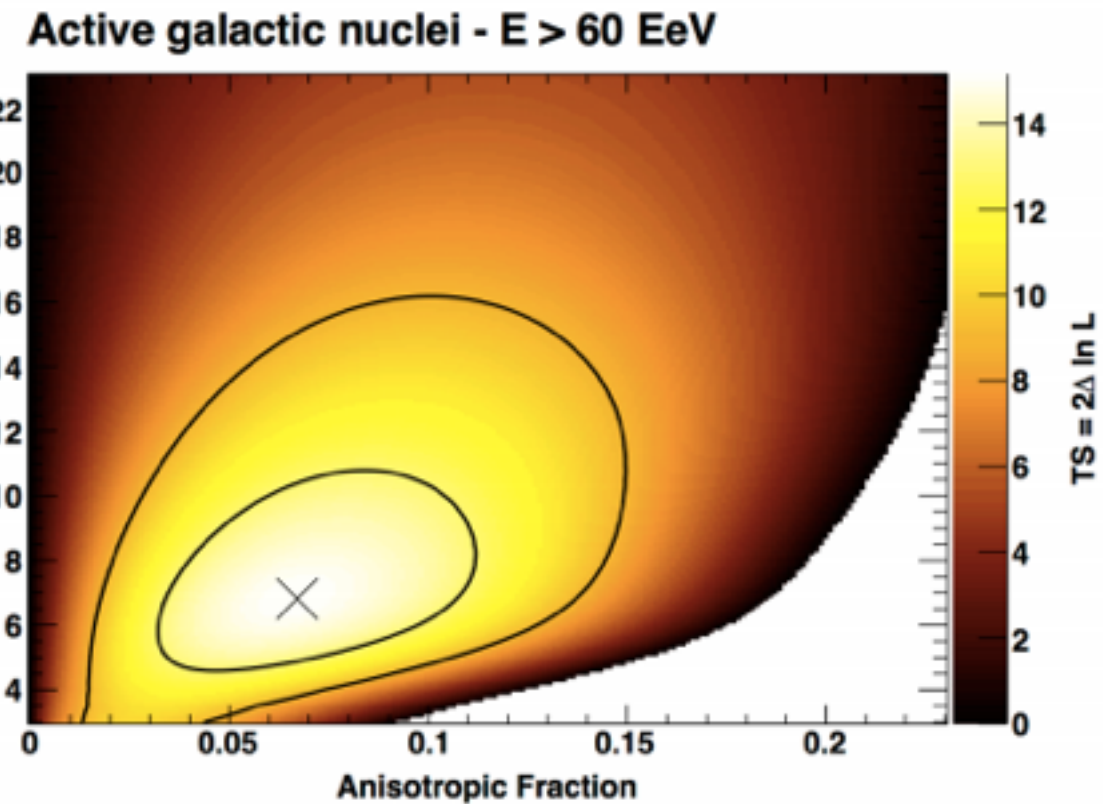
$$f_{\text{ani}} = 10\%, \Psi = 13^{\circ}$$

$$\text{TS} = 24.9 \longrightarrow p\text{-value } 3.8 \times 10^{-6}$$

## Post-trial probability

$$3.6 \times 10^{-5} (\sim 4 \sigma)$$

(fraction of isotropic simulations that have a greater TS under the same energy scan)



## $\gamma$ -ray detected AGNs

$$f_{\text{ani}} = 7\%, \Psi = 7^{\circ}$$

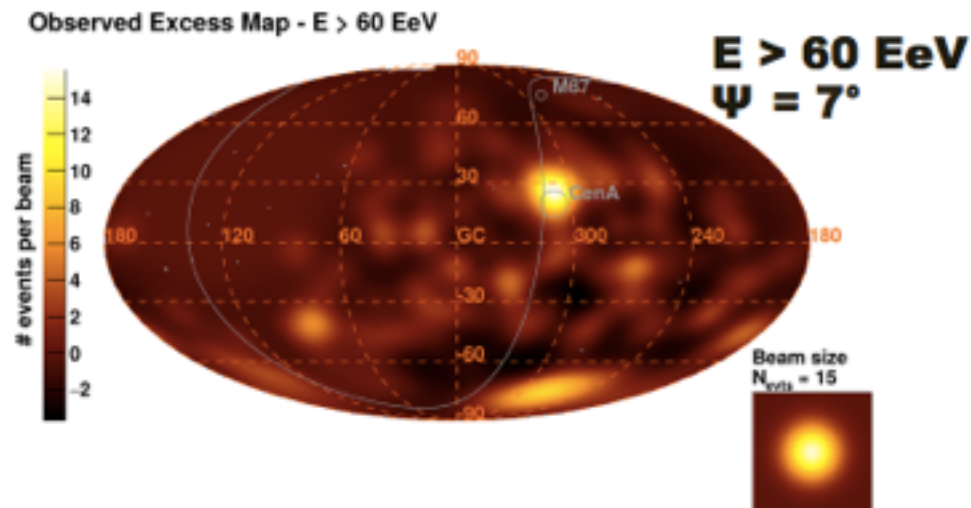
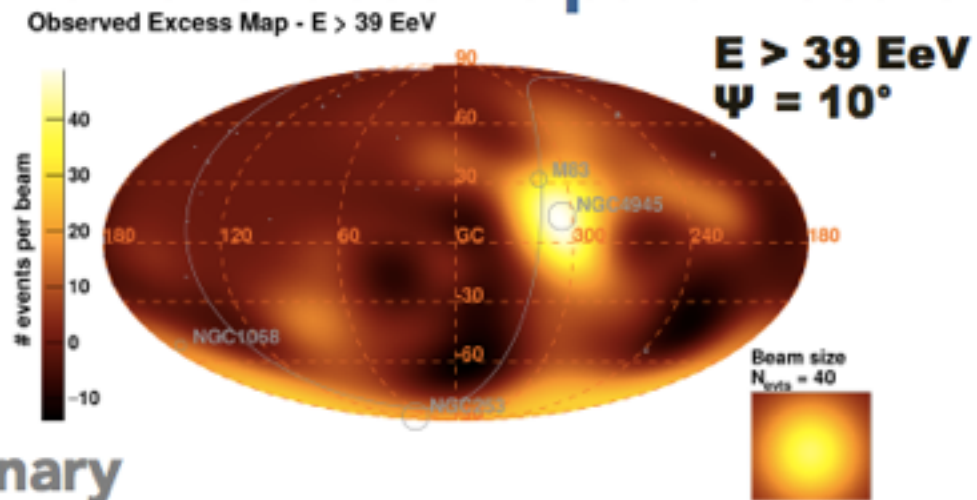
$$\text{TS} = 15.2 \longrightarrow p\text{-value } 5.1 \times 10^{-4}$$

## Post-trial probability

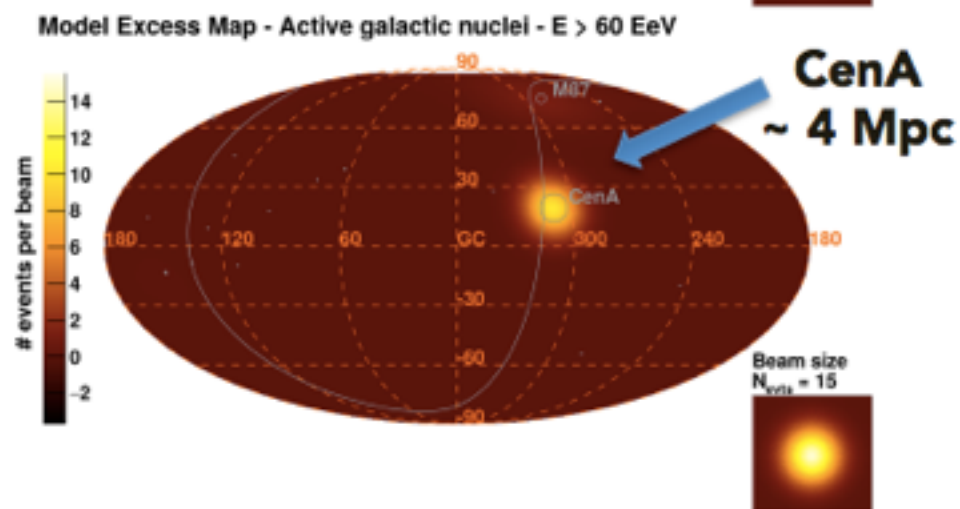
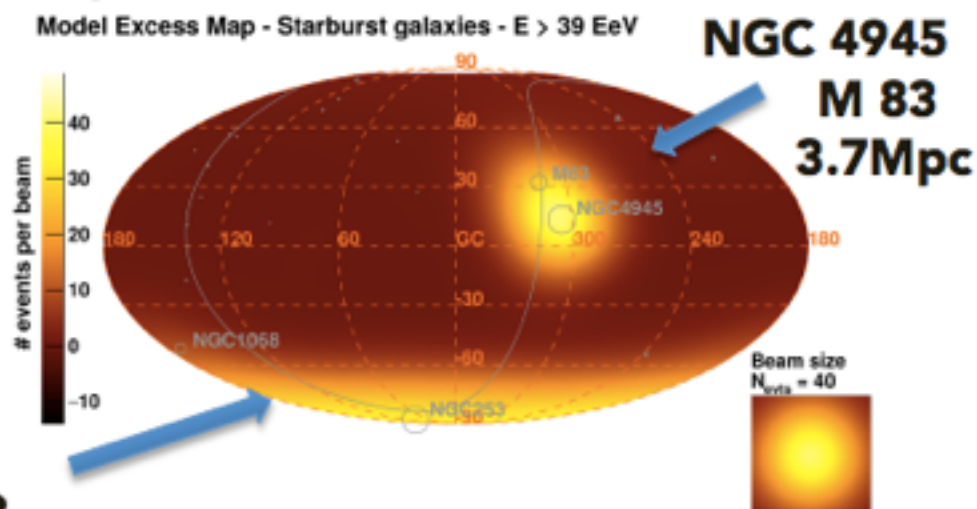
$$3 \times 10^{-3} (\sim 2.7 \sigma)$$

# Best fit and residual maps (through Auger f.o.v.)

## Maps for the best-fit parameters

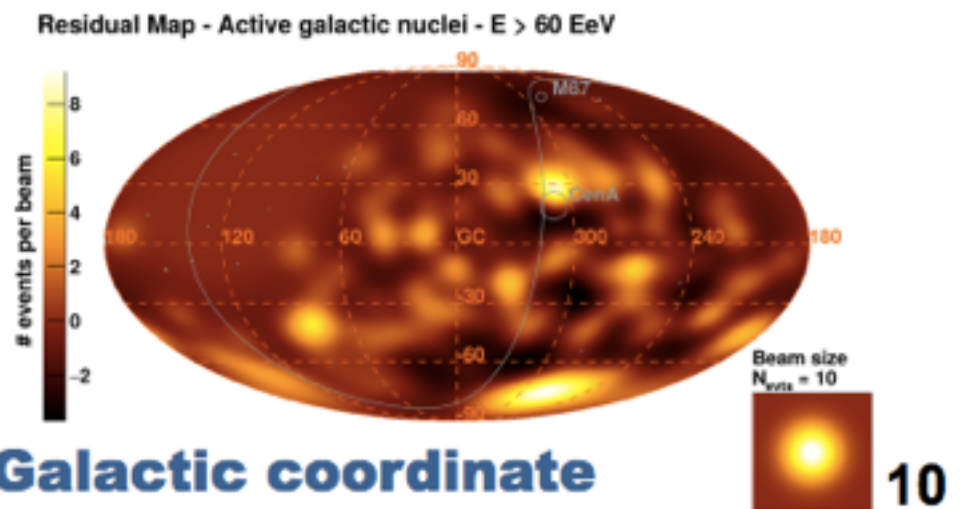
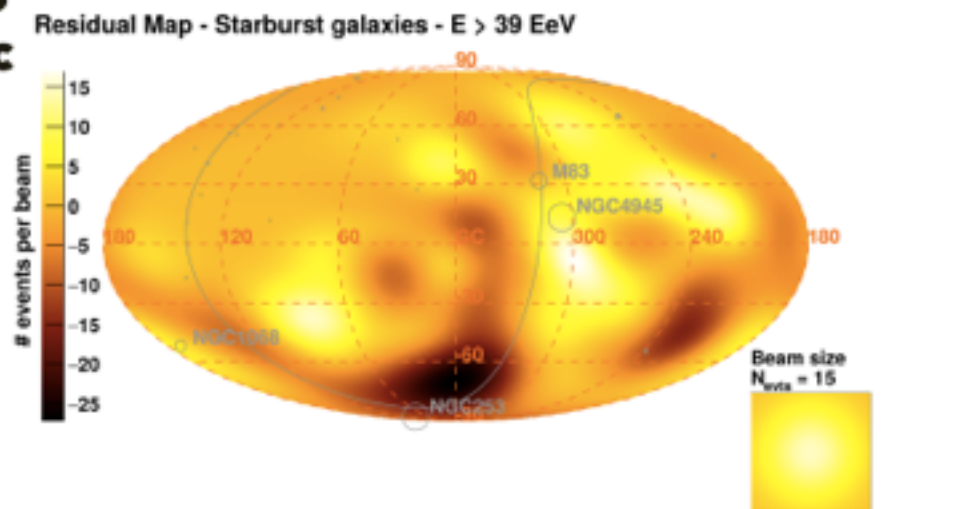


preliminary



NGC 253  
2.5 Mpc

NGC 1068  
16.7 Mpc



Galactic coordinate

10

# SBGs vs $\gamma$ -AGNs

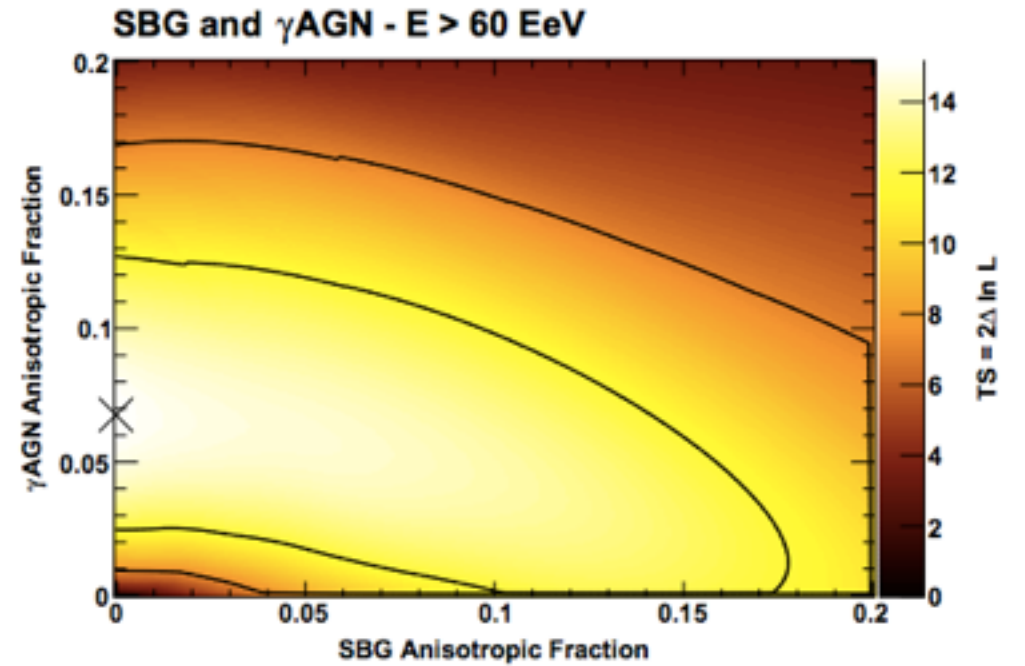
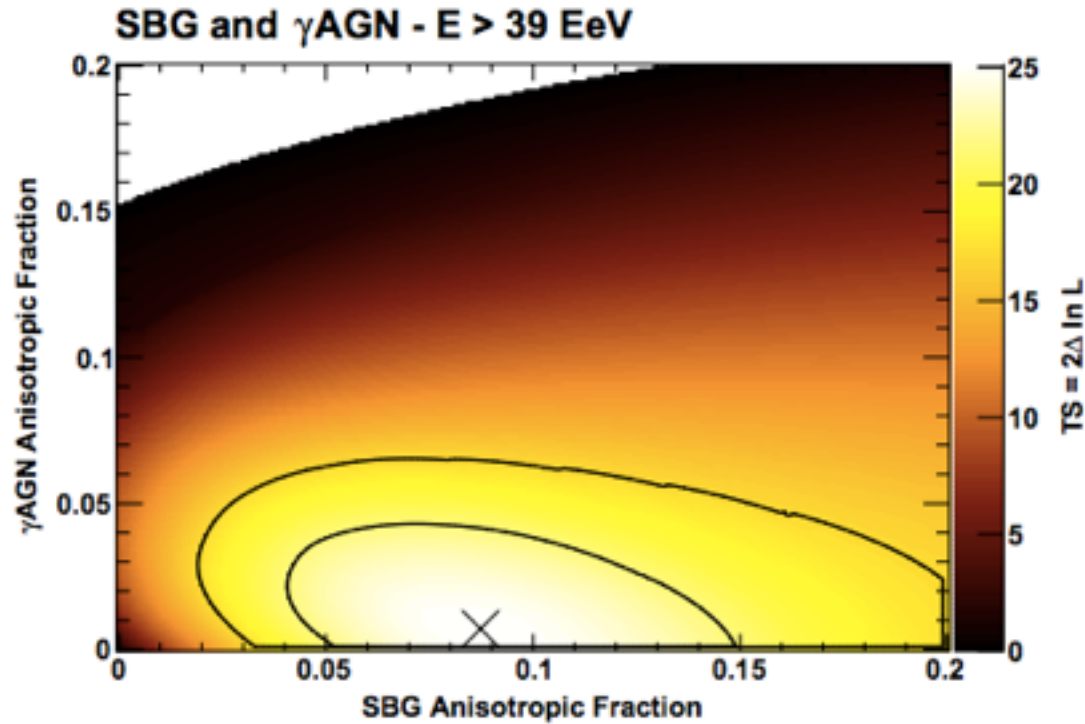
**Table 1.** Results obtained above 39 EeV and 60 EeV

Test hypothesis	Null hypothesis	Threshold energy <sup>a</sup>	TS	Local p-value $\mathcal{P}_{\chi^2}(\text{TS}, 2)$	Post-trial p-value	1-sided significance	AGN fraction	SB fraction	Search radius
SBG + ISO	ISO	39 EeV	24.9	$3.8 \times 10^{-6}$	$3.6 \times 10^{-5}$	$4.0 \sigma$	N/A	9.7%	$12.9^\circ$
$\gamma$ AGN + ISO	ISO	39 EeV	10.4	$5.4 \times 10^{-3}$	N/A	N/A	3.8%	N/A	$10.0^\circ$
$\gamma$ AGN + SBG + ISO	SBG + ISO	39 EeV	0.2	N/A	0.66	$-0.4 \sigma$	0.7%	8.7%	$12.5^\circ$
$\gamma$ AGN + SBG + ISO	$\gamma$ AGN + ISO	39 EeV	14.7	N/A	$1.3 \times 10^{-4}$	$3.7 \sigma$	0.7%	8.7%	$12.5^\circ$
$\gamma$ AGN + ISO	ISO	60 EeV	15.2	$5.1 \times 10^{-4}$	$3.1 \times 10^{-3}$	$2.7 \sigma$	6.7%	N/A	$6.9^\circ$
SBG + ISO	ISO	60 EeV	12.2	$2.5 \times 10^{-3}$	N/A	N/A	N/A	13.7%	$12.0^\circ$
$\gamma$ AGN + SBG + ISO	$\gamma$ AGN + ISO	60 EeV	0.003	N/A	0.96	$-1.7 \sigma$	6.8%	0.0% <sup>b</sup>	$7.0^\circ$
$\gamma$ AGN + SBG + ISO	SBG + ISO	60 EeV	3.0	N/A	0.08	$1.4 \sigma$	6.8%	0.0% <sup>b</sup>	$7.0^\circ$

<sup>a</sup>For composite model studies, no scan over the threshold energy is performed.

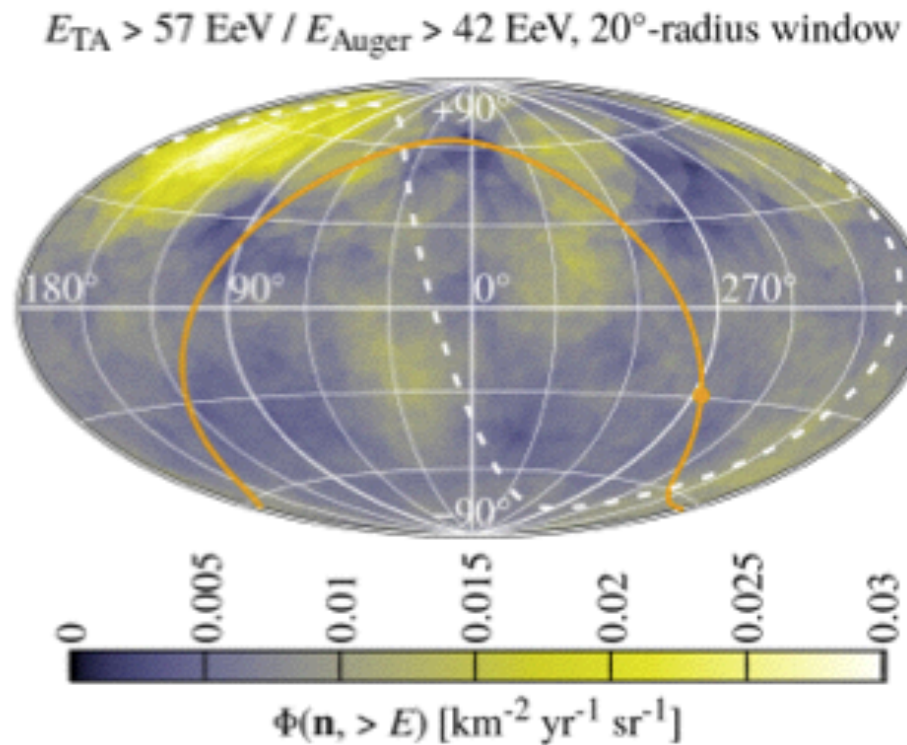
<sup>b</sup>Maximum TS reached at the boundary of the parameter space.

ISO: isotropic model.



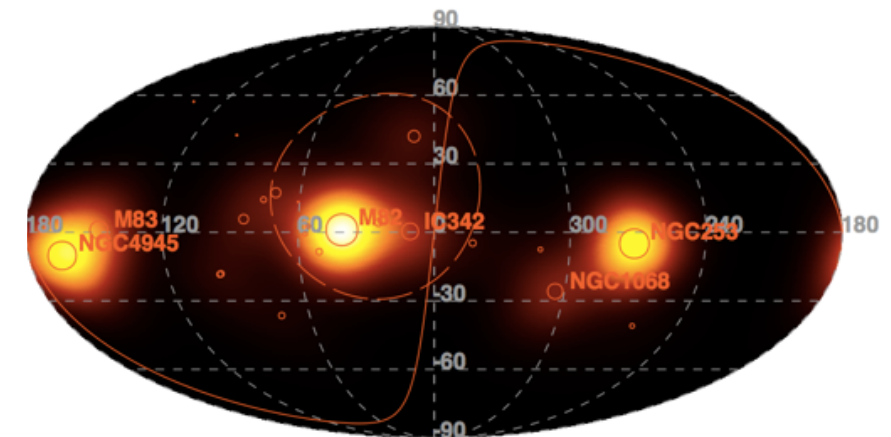
# Perspectives

- Full-sky survey



[Auger/TA coll., UHECR16]

Flux Map - Starburst galaxies -  $E > 39 \text{ EeV}$

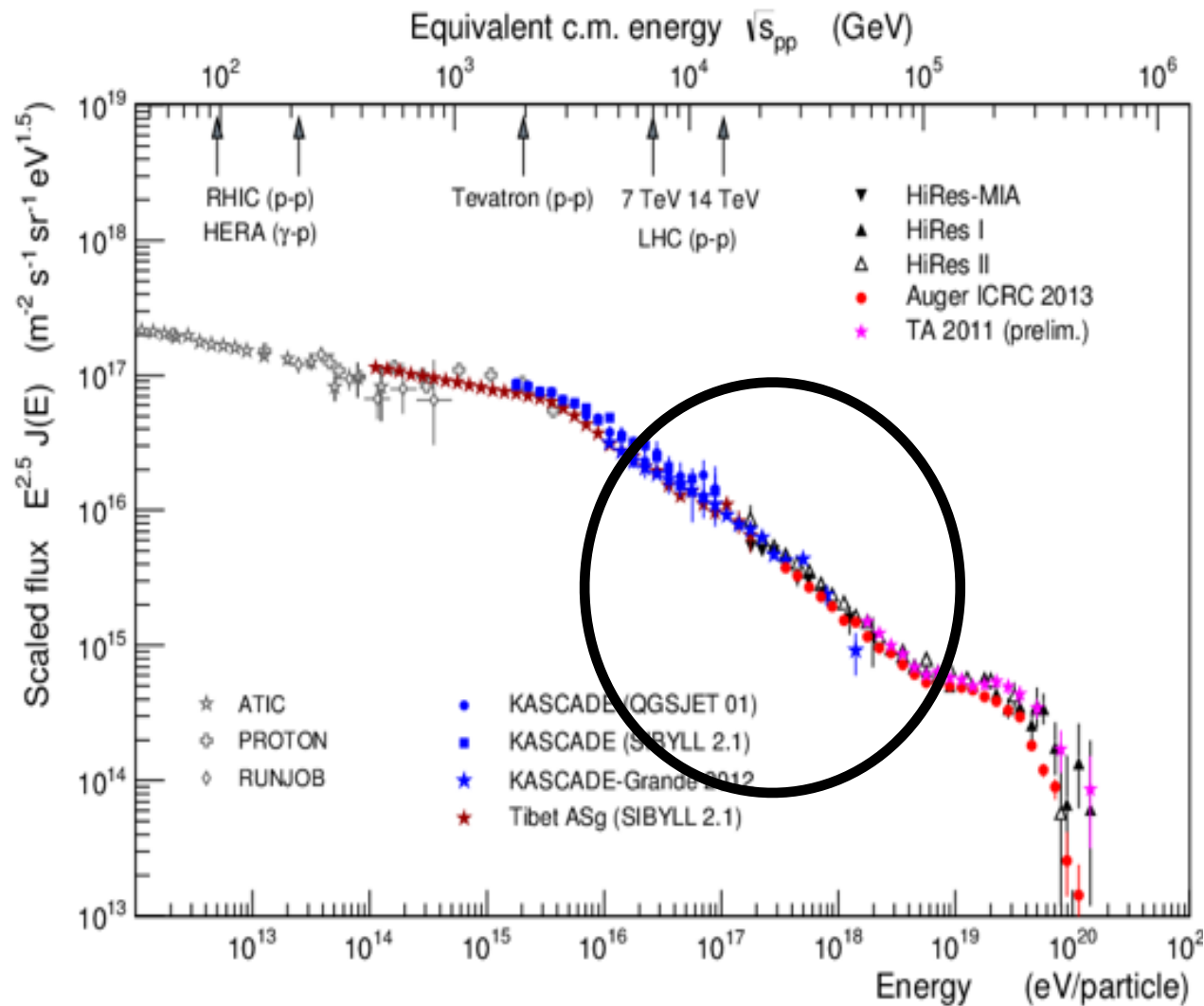


- Include galactic magnetic models in the picture
- Rigidity-dependent analyses — upgrade of the Auger Observatory
- Global picture spectrum/mass/anisotropies?

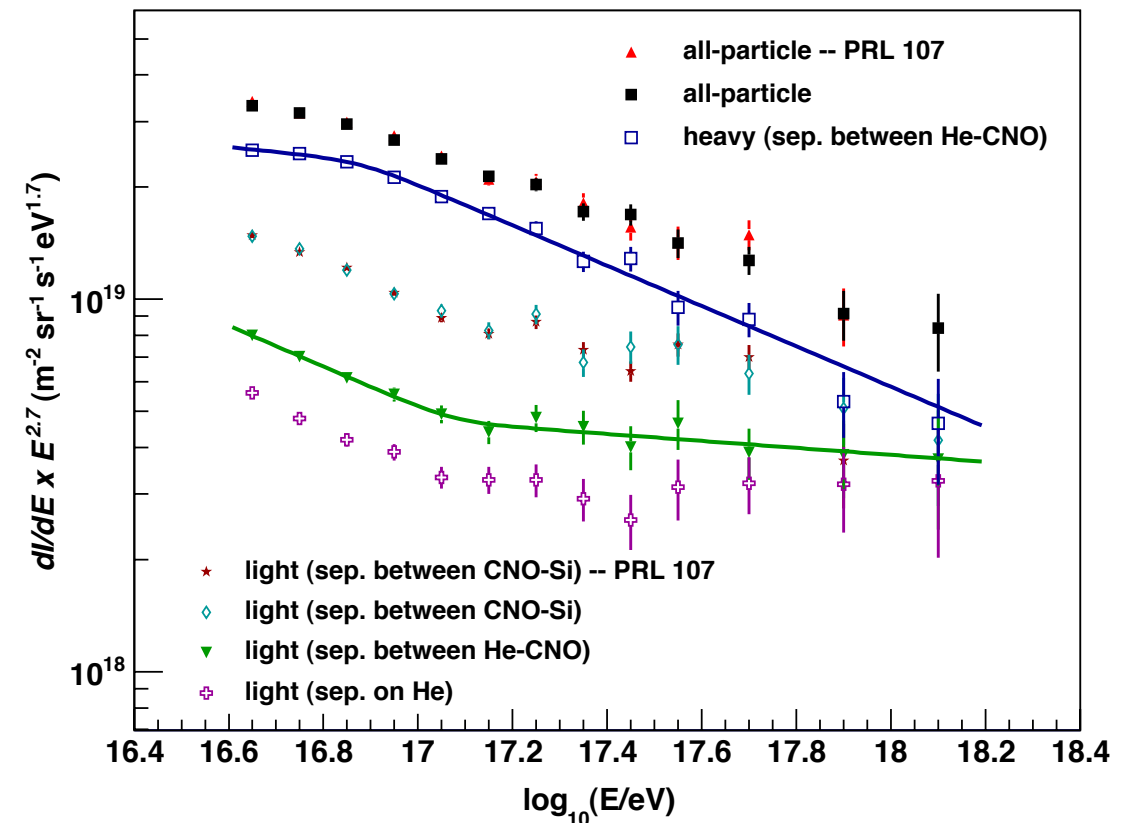


*vi)* **Backup**

# End of Galactic CRs

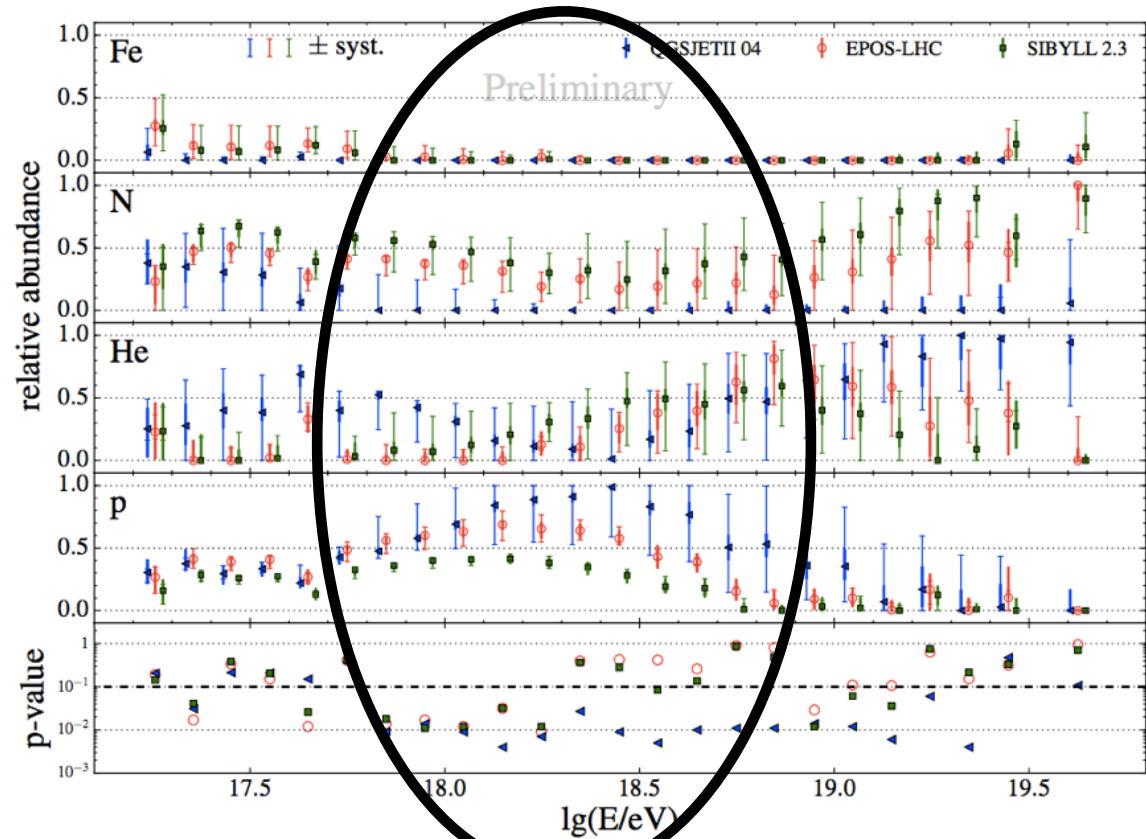


PHYSICAL REVIEW D 87, 081101(R) (2013)



- Rigidity-dependent scenario for GCRs
- « Knees » = maximum acceleration energies
- Extragalactic protons entering progressively

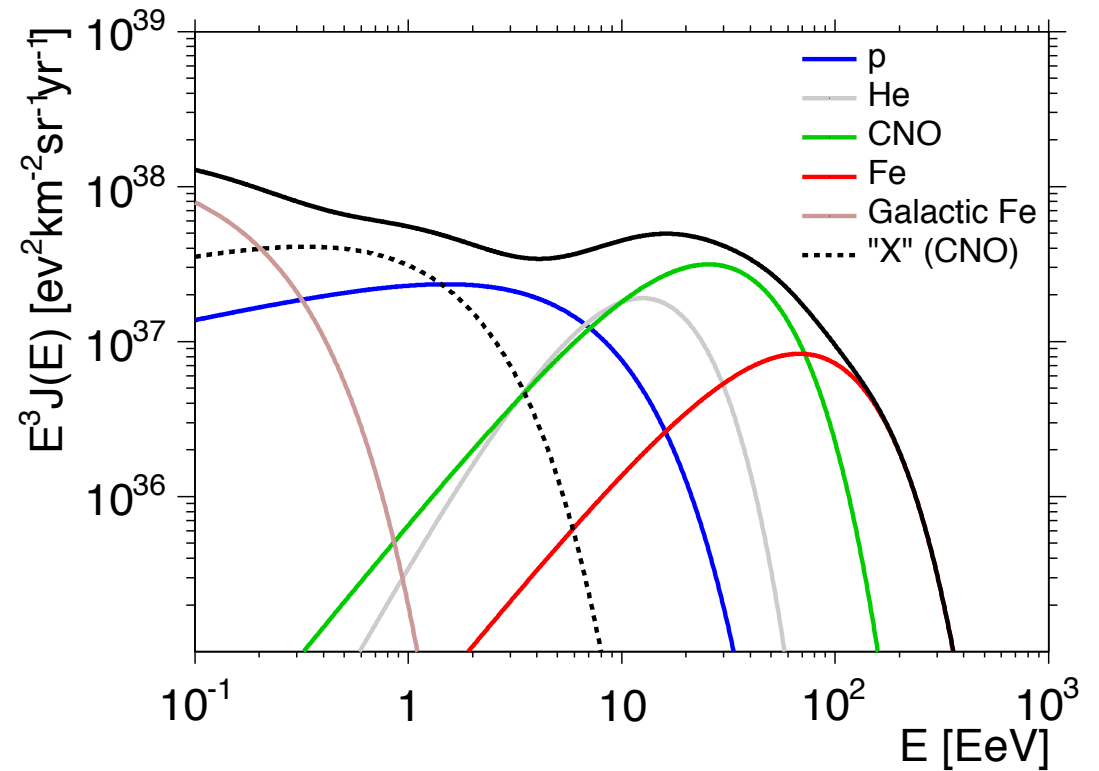
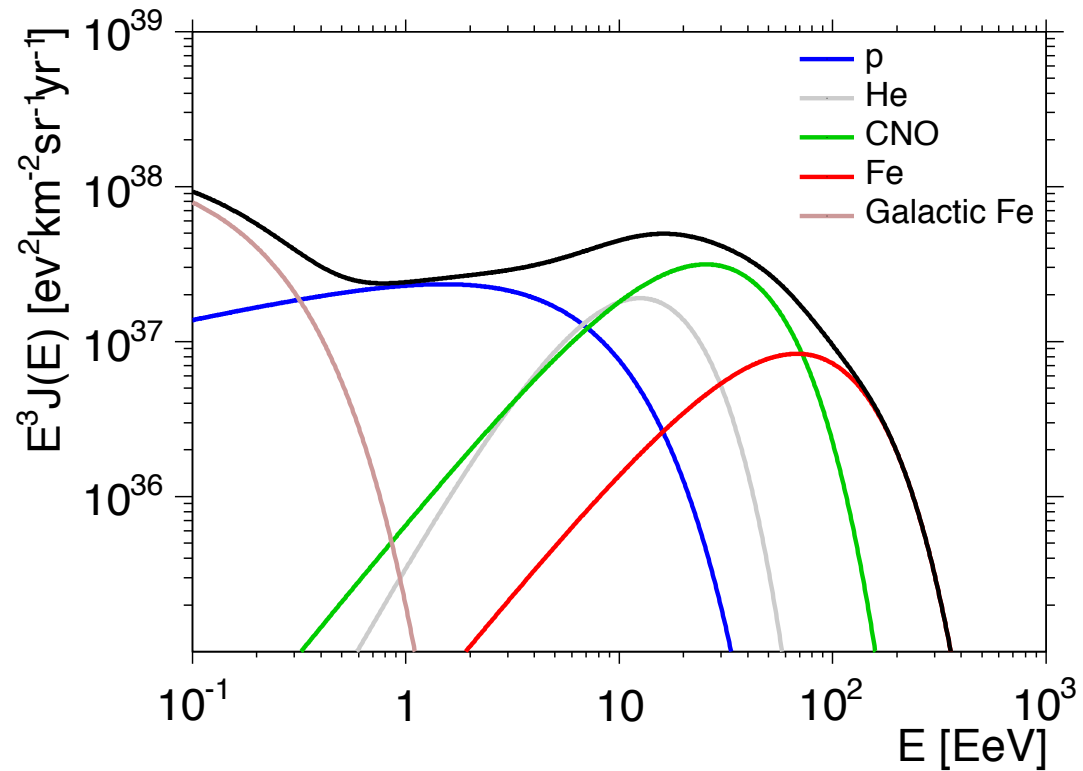
# The Ankle?



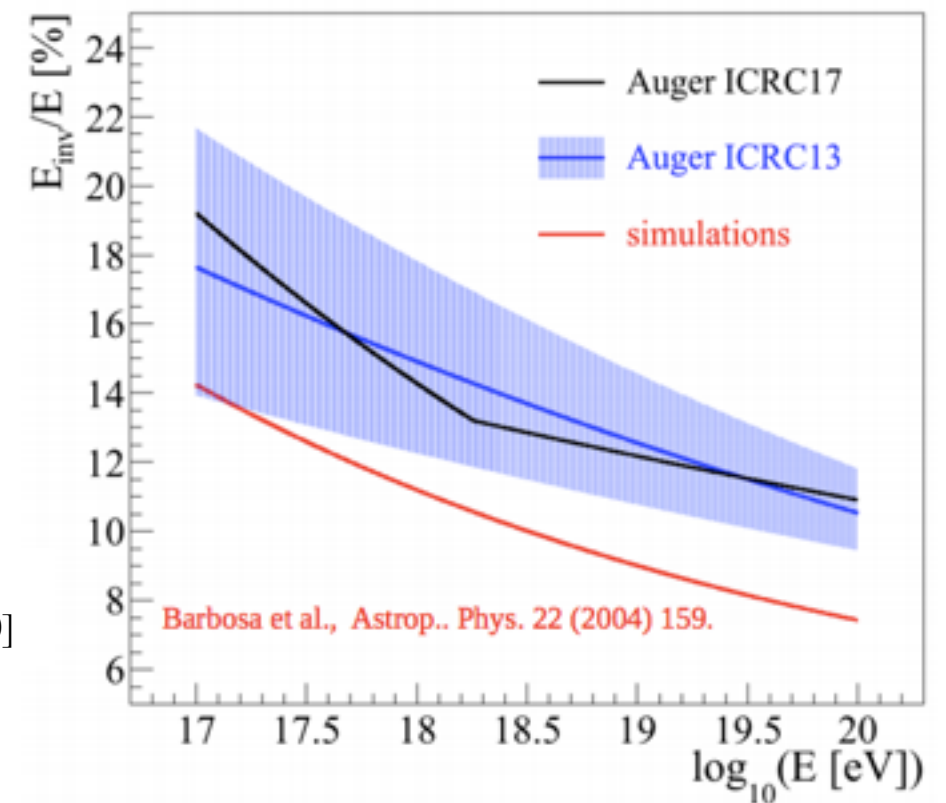
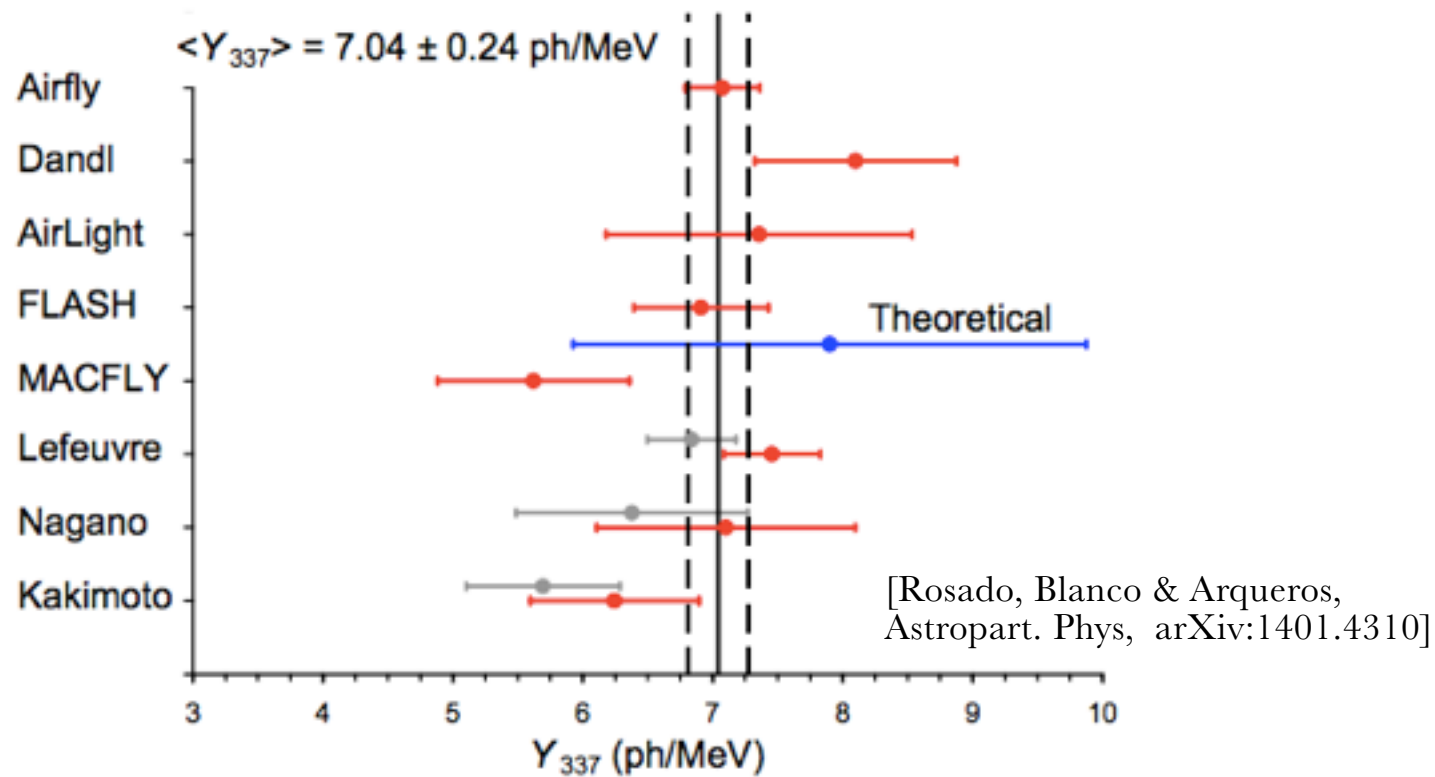
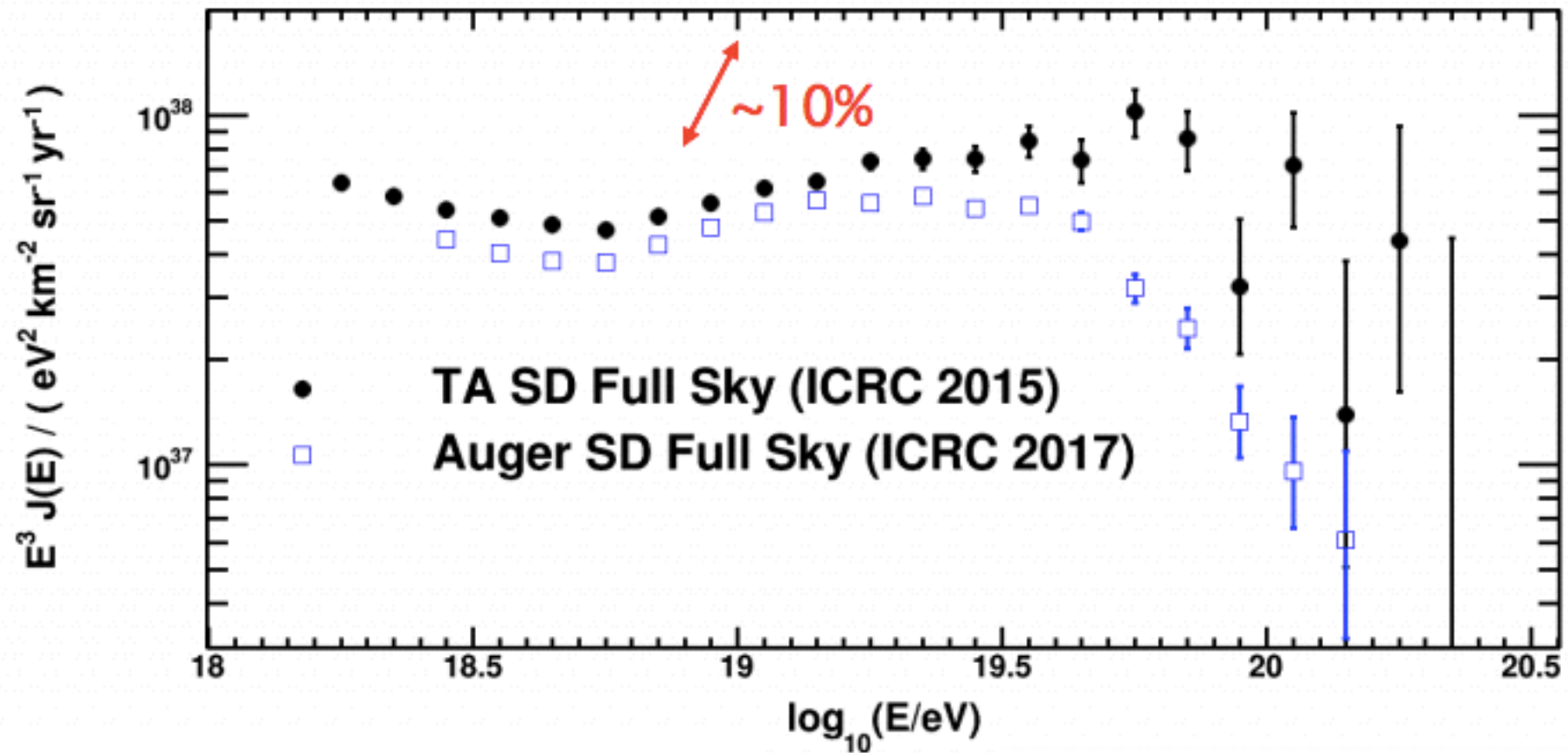
Gal/xGal scenario

➔ In addition to (extragalactic) protons, EeV CRs are from the CNO group, not Fe!

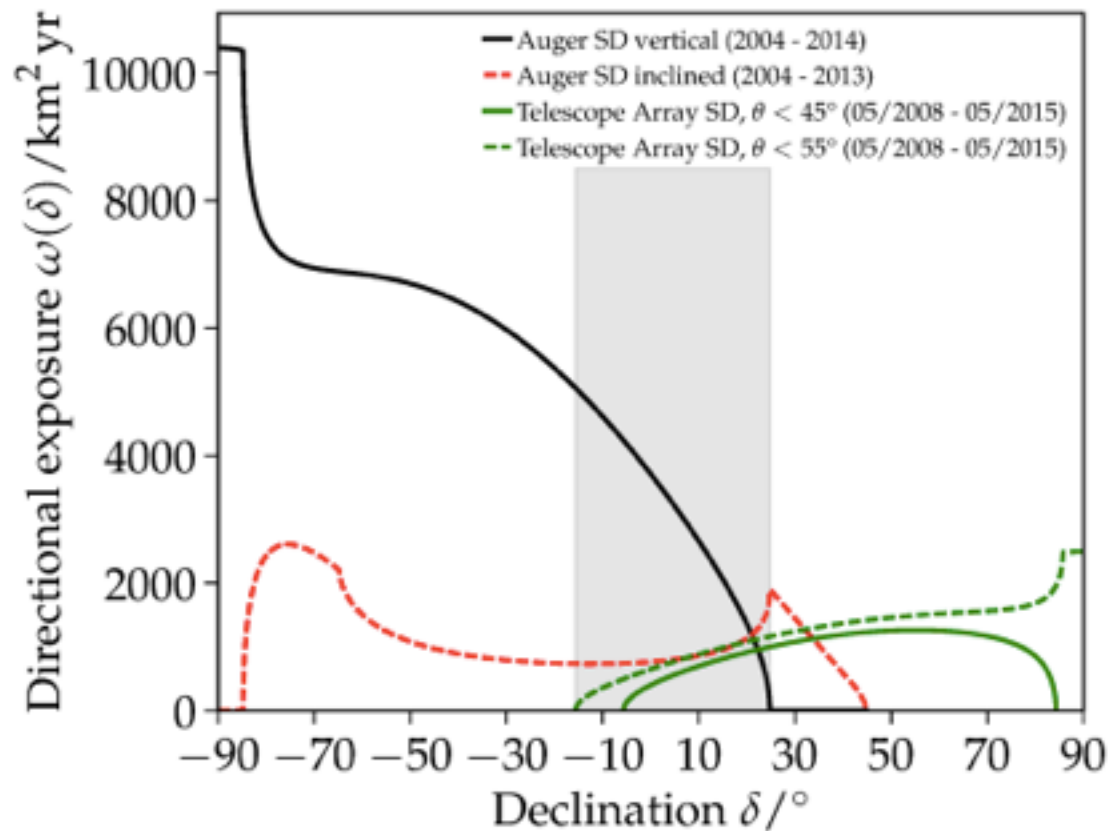
Observed scenario



# Energy spectrum: Auger vs Telescope Array



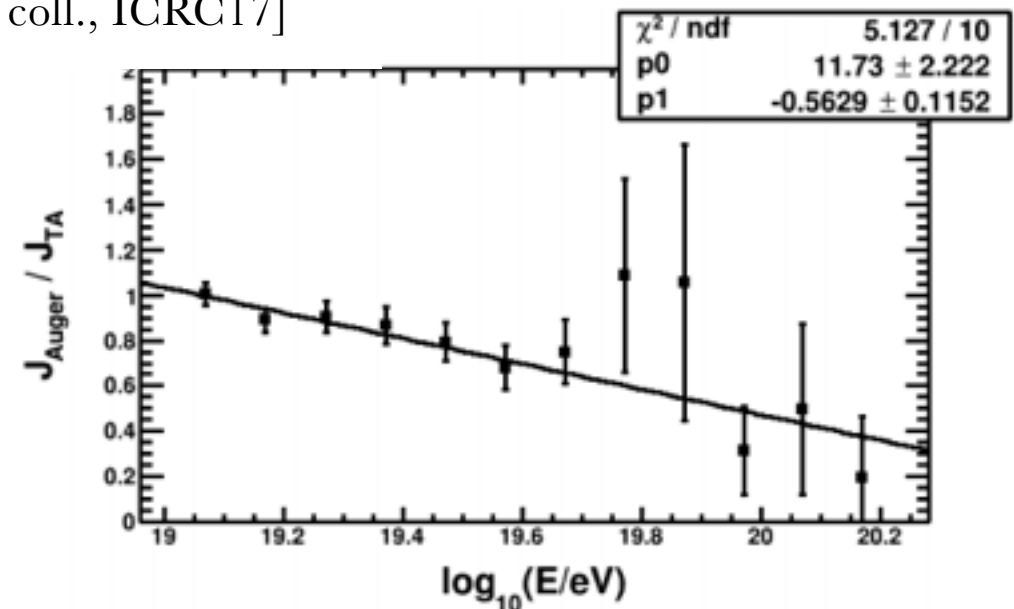
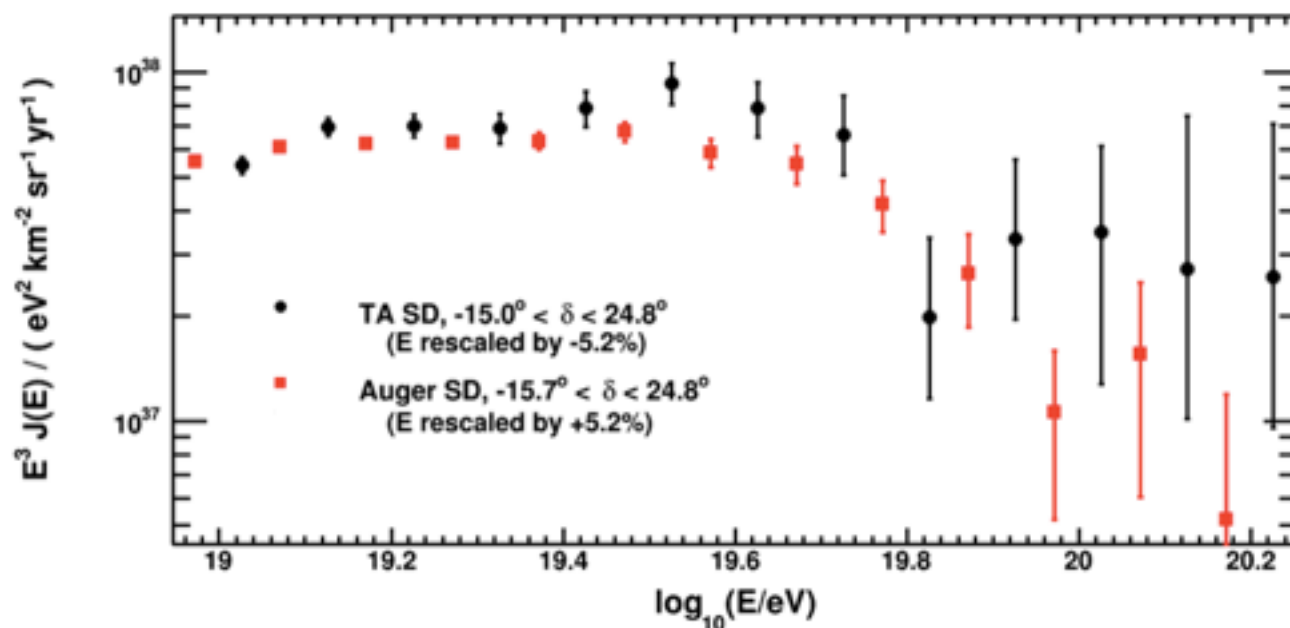
# Auger vs Telescope Array: common sky



$$J_{1/\omega}(E) = \frac{1}{\Delta\Omega\Delta E} \sum_{i=1}^N \frac{1}{\omega(\delta_i)}$$

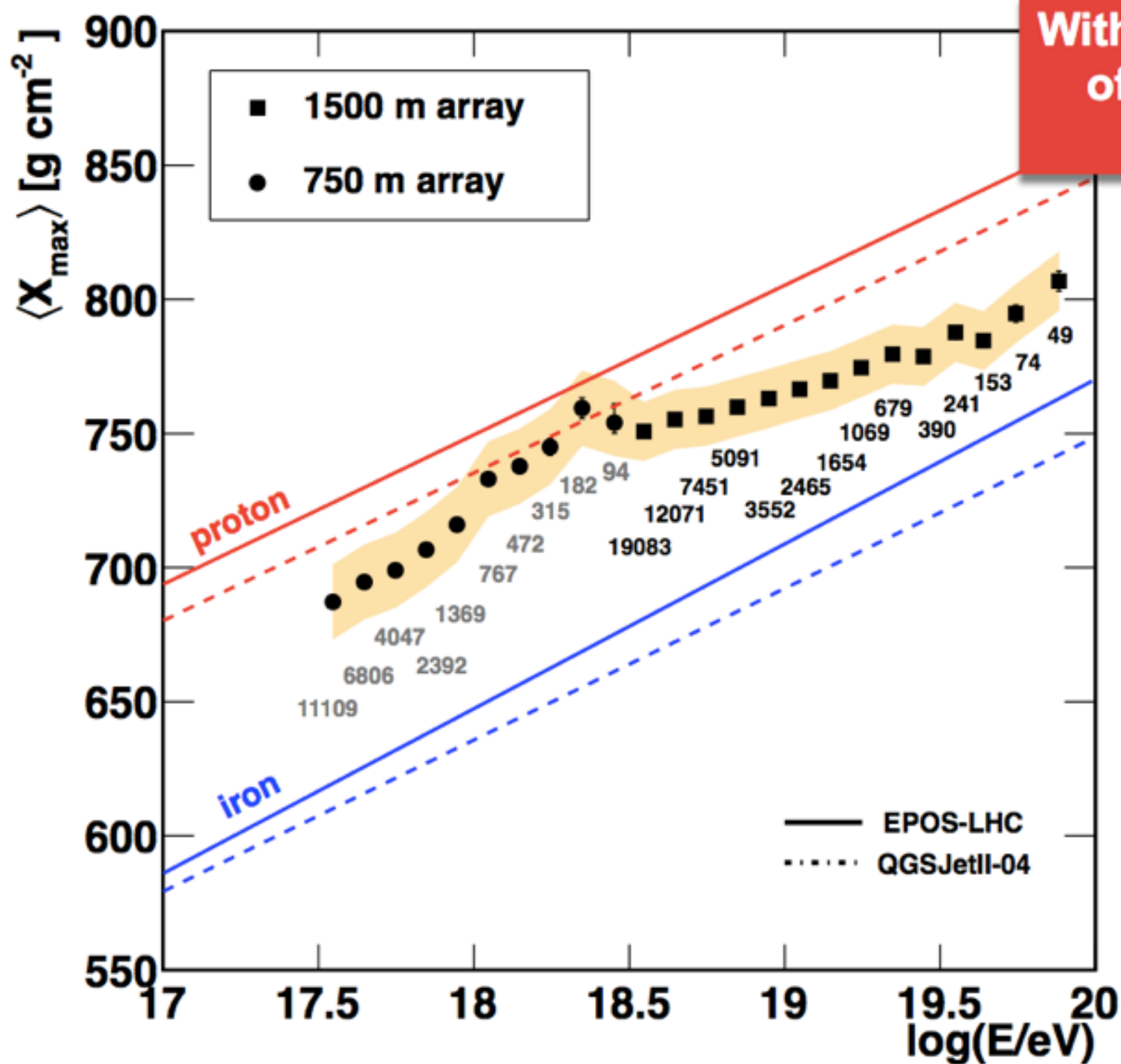
➔ Remove distortions induced from different directional exposures in case of anisotropies

[Ivanov for Auger/TA coll., ICRC17]



➔ Energy-dependent systematics...

# $\langle X_{\max} \rangle$ with SD events



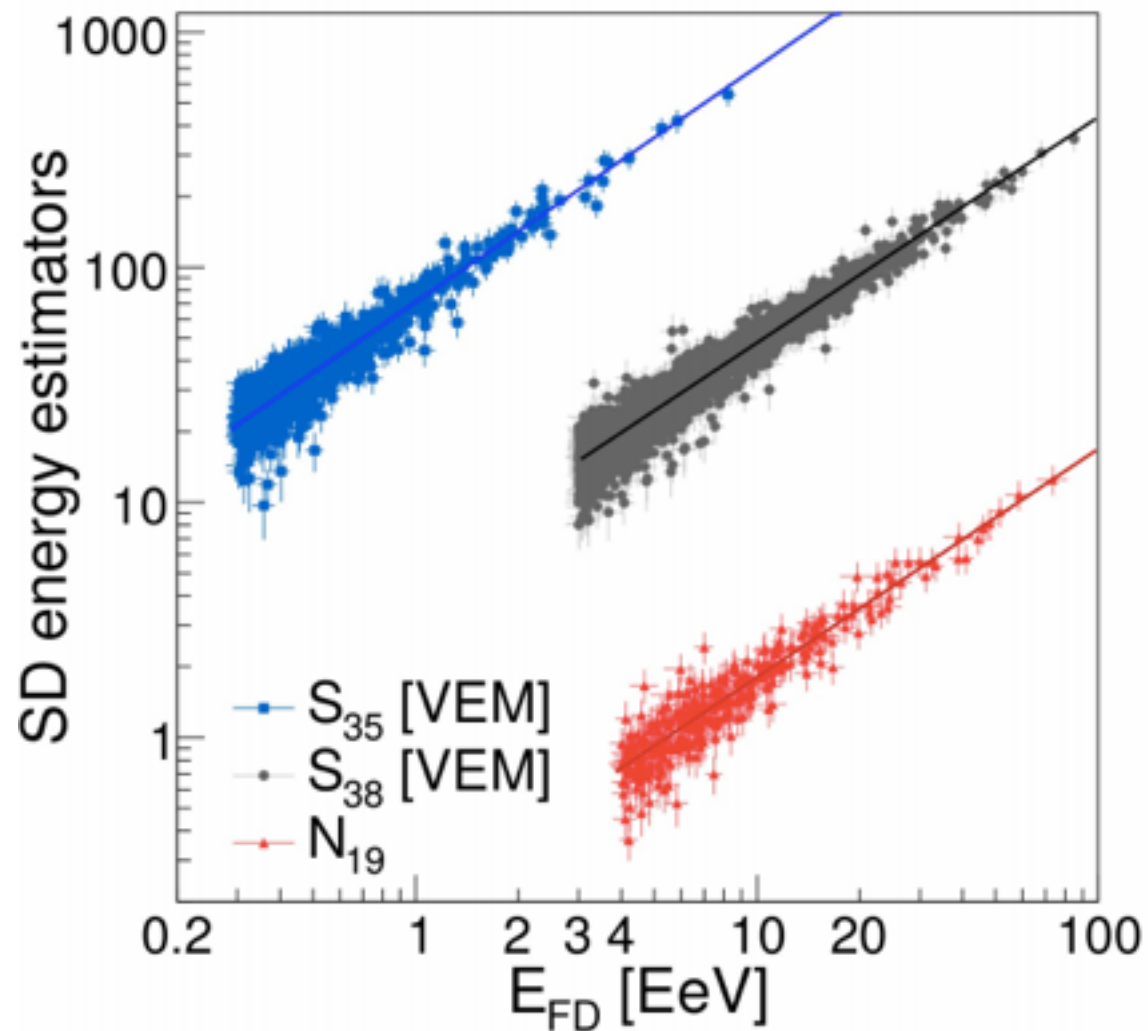
With the SD we obtain a measurement of  $\langle X_{\max} \rangle$  that covers more than 2 orders of magnitude in energy

- Systematics 11-14  $\text{g cm}^{-2}$
- First composition analysis with data of the 750 m array
- We add 3 energy bins at the highest energies compared to the FD

This SD analysis has 517 events above  $10^{19.5}$  eV, nearly 10 times more events than the FD measurements in this energy range

# SD-energy calibration

Measurement of the attenuation through ‘constant intensity cut’



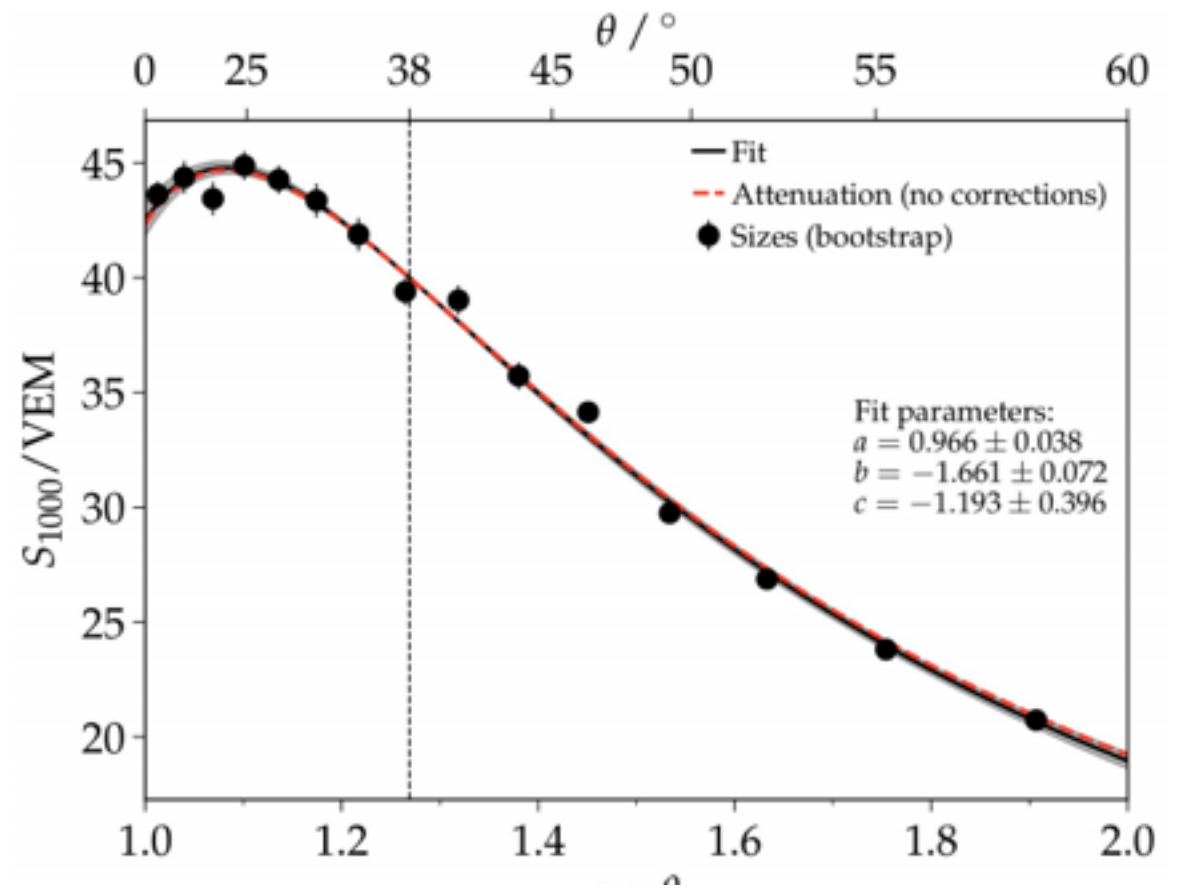
**Resolution:**

SD-1500 ~ 15%

SD-1500 inclined ~ 17%

SD-750 ~ 13%

FD ~ 7%



High quality hybrid events

(2661 events for  $S_{38}$ )

$$E_{FD} = A \hat{S}^B$$

$$\hat{S} = S_{38}, S_{35}, N_{19}$$